SAND2020-3809PE

Material Properties of Liquid Iron at Planetary Core Conditions

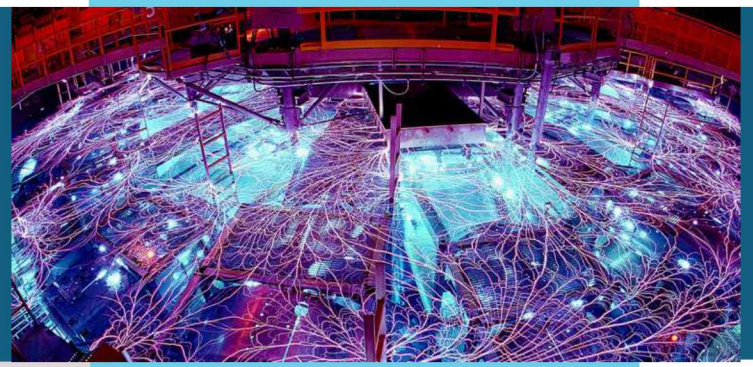

Sean Grant, PhD Defense

Contributing Scientists:

University of Texas: Todd Ditmire, Jung-Fu Lin, Aaron Bernstein

Sandia National Laboratories: Tommy Ao, Kyle Cochrane, Jean-Paul Davis, Daniel Dolan, Andrew Porwitzky, Christopher Seagle, John Benage, Dawn Flicker

Sandia National Laboratories is a multimission laboratory managed and operated by National Technology & Engineering Solutions of Sandia, LLC, a wholly owned subsidiary of Honeywell International Inc., for the U.S. Department of Energy's National Nuclear Security Administration under contract DE-NA0003525.

Iron is an important material for planetary sciences and many other high energy density applications

Important Current Research:

- Measuring the P-ρ equation of state (EOS) of liquid iron at previously unexplored off-Hugoniot isentropes
- Isentropic compression is an extremely useful way to study planetary equations of state

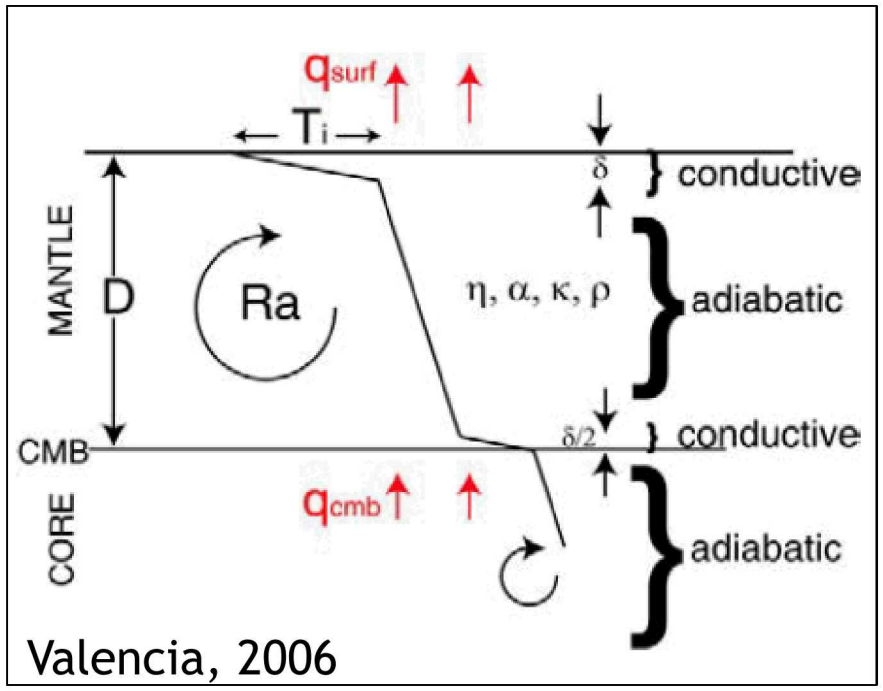

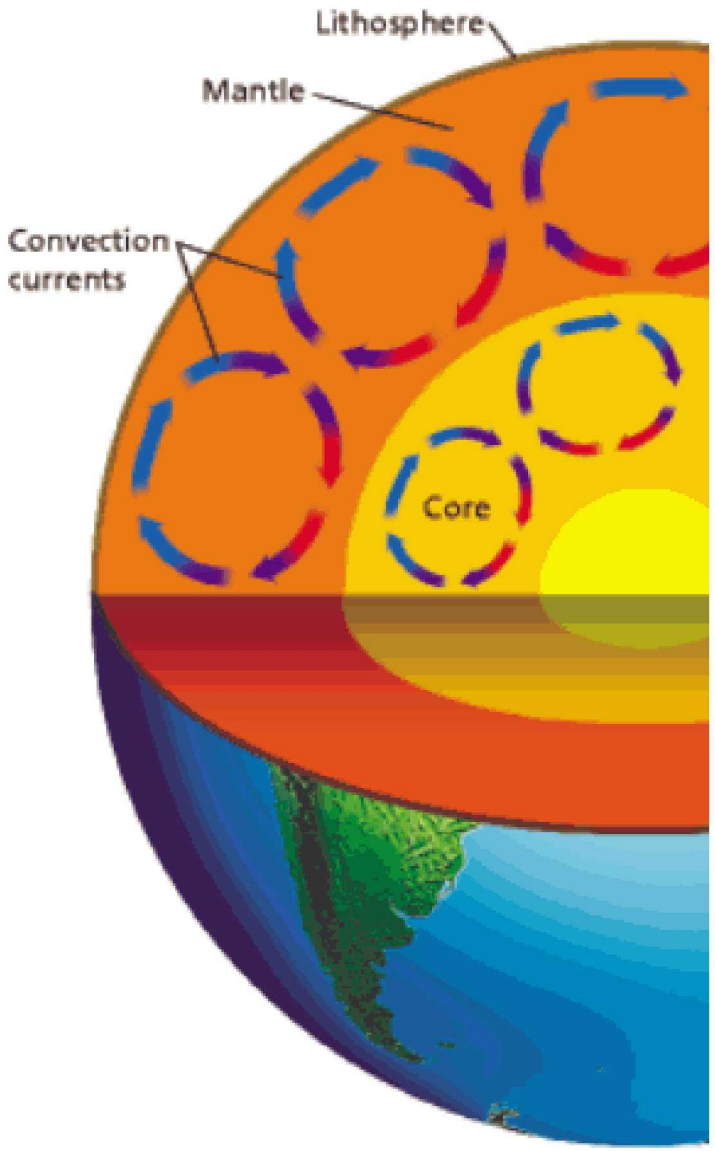

The conductivity of iron is important for understanding the evolution of planetary cores

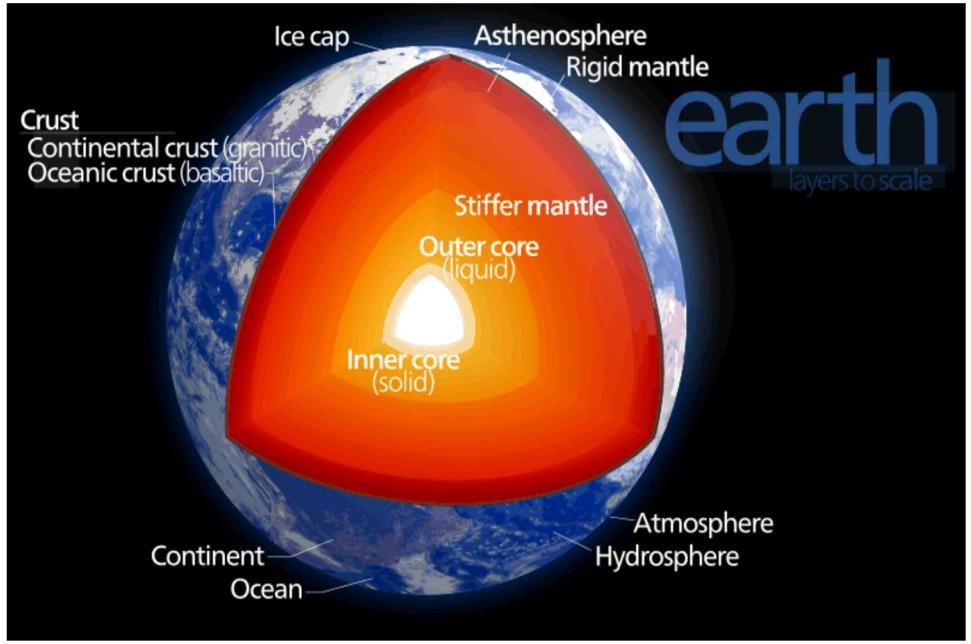

Convection drives the magnetic field

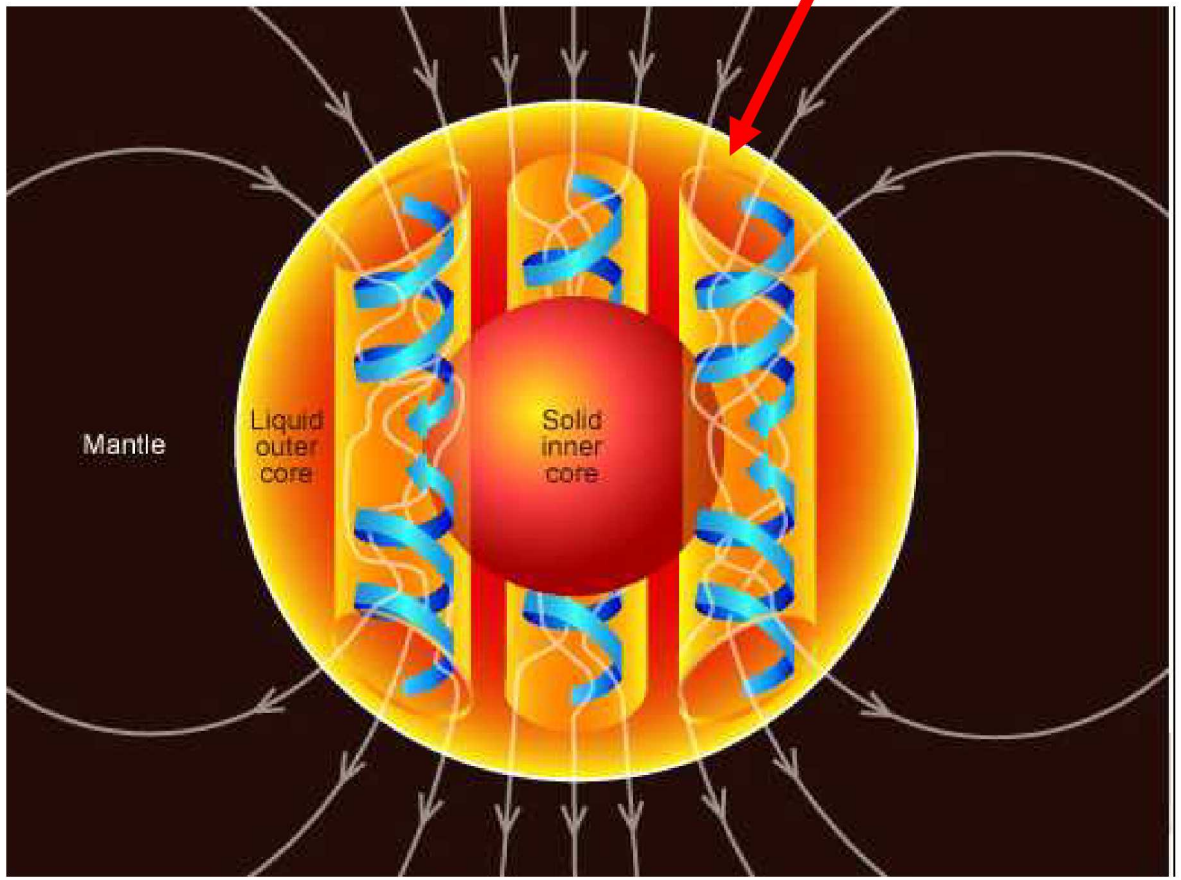

Unresolved Question:

- Current estimates of the conductivity of the Earth's core could produce an inner core ranging from 4 billion to 1 billion years old

Important Current Research:

- Measuring conductivity of liquid iron at planetary core conditions

We designed an experimental path close to the conditions of the Earth's core

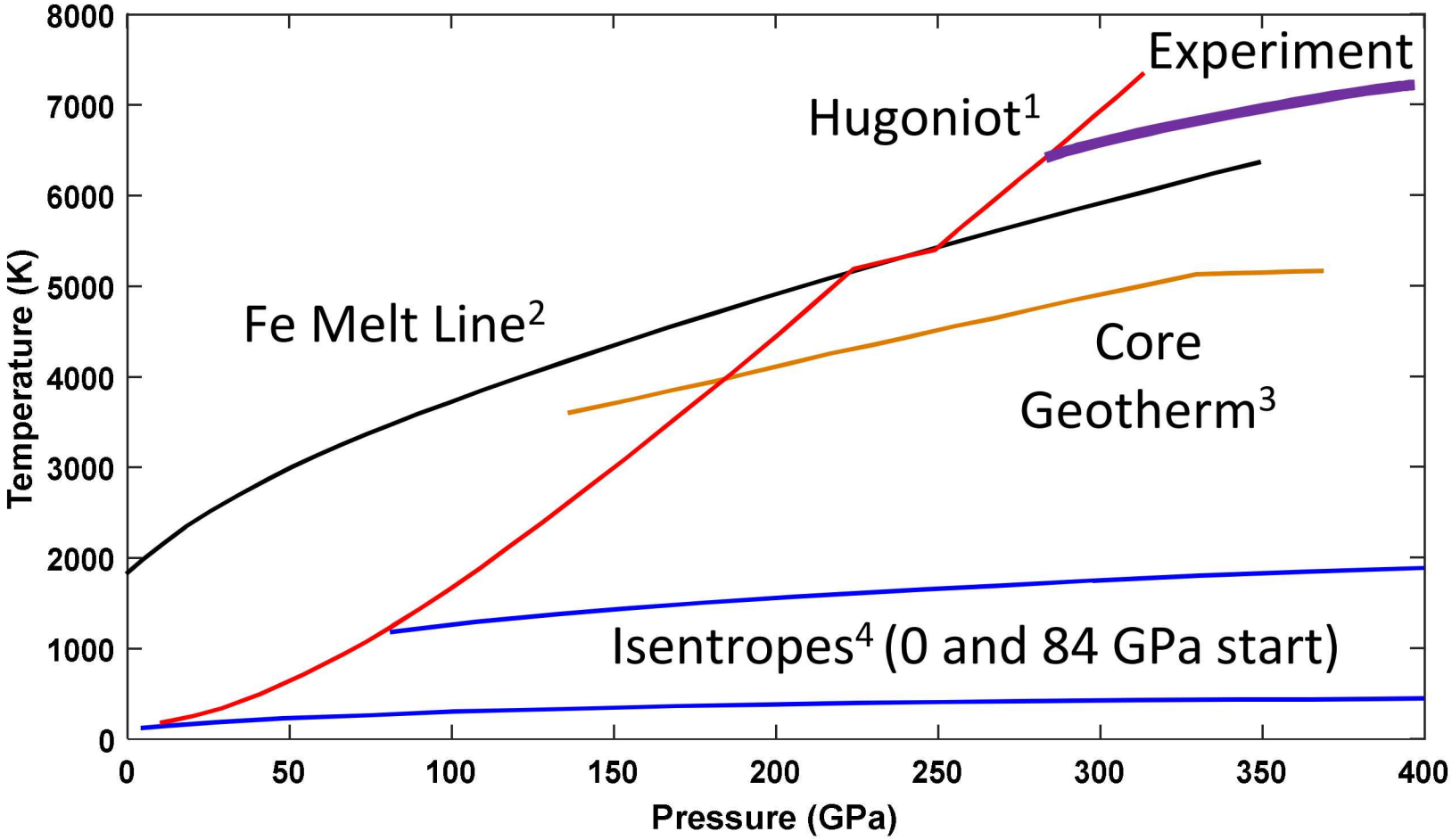

[1]J. M. Brown and R. G. McQueen, J. Geophys. Res. 91, 7485, doi:10.1029/ JB091iB07p07485 (1986).
[2]S. Anzellini, A. Dewaele, M. Mezouar, P. Loubeyre, & G. Morard, (2013). Science, 340(6131), 464-466.
[3]F. D. Stacey, *Physics of the Earth*, 4th ed. (Cambridge University Press, Cambridge, 2008).
[4]J. Wang, R. F. Smith, J. H. Eggert, D. G. Braun, T. R. Boehly, J. Reed Patterson, P. M. Celliers, R. Jeanloz, G. W. Collins, and T. S. Duffy. Journal of Applied Physics, 114(2), p.023513. doi.:10.1063/1.4813091 (2013).

The strip-line target configuration is a common method of driving planar samples to high pressure and density states on Z

Load hardware details

- Top Sample Pair Shown
- Parallel counter-propagating current drives the panels apart symmetrically
- Flight gap leads to initial shock

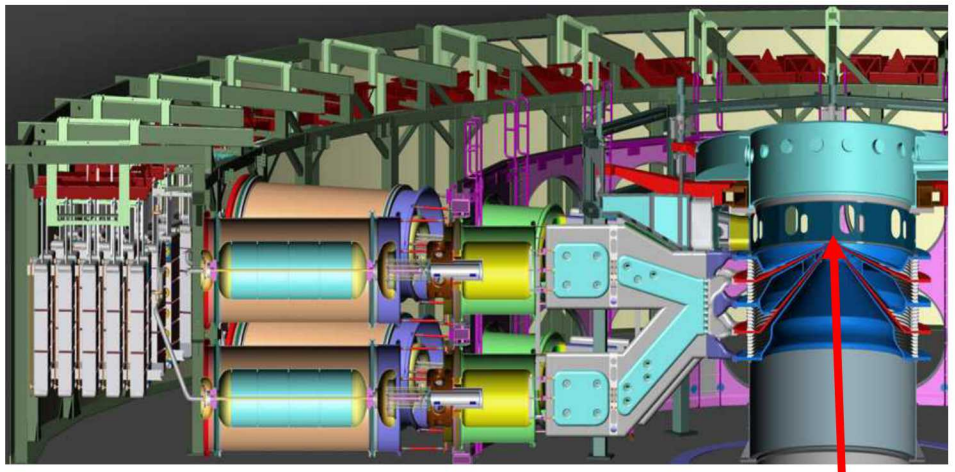

Marx Banks

Triggering and Pulse Shaping

Center Section: Load Hardware

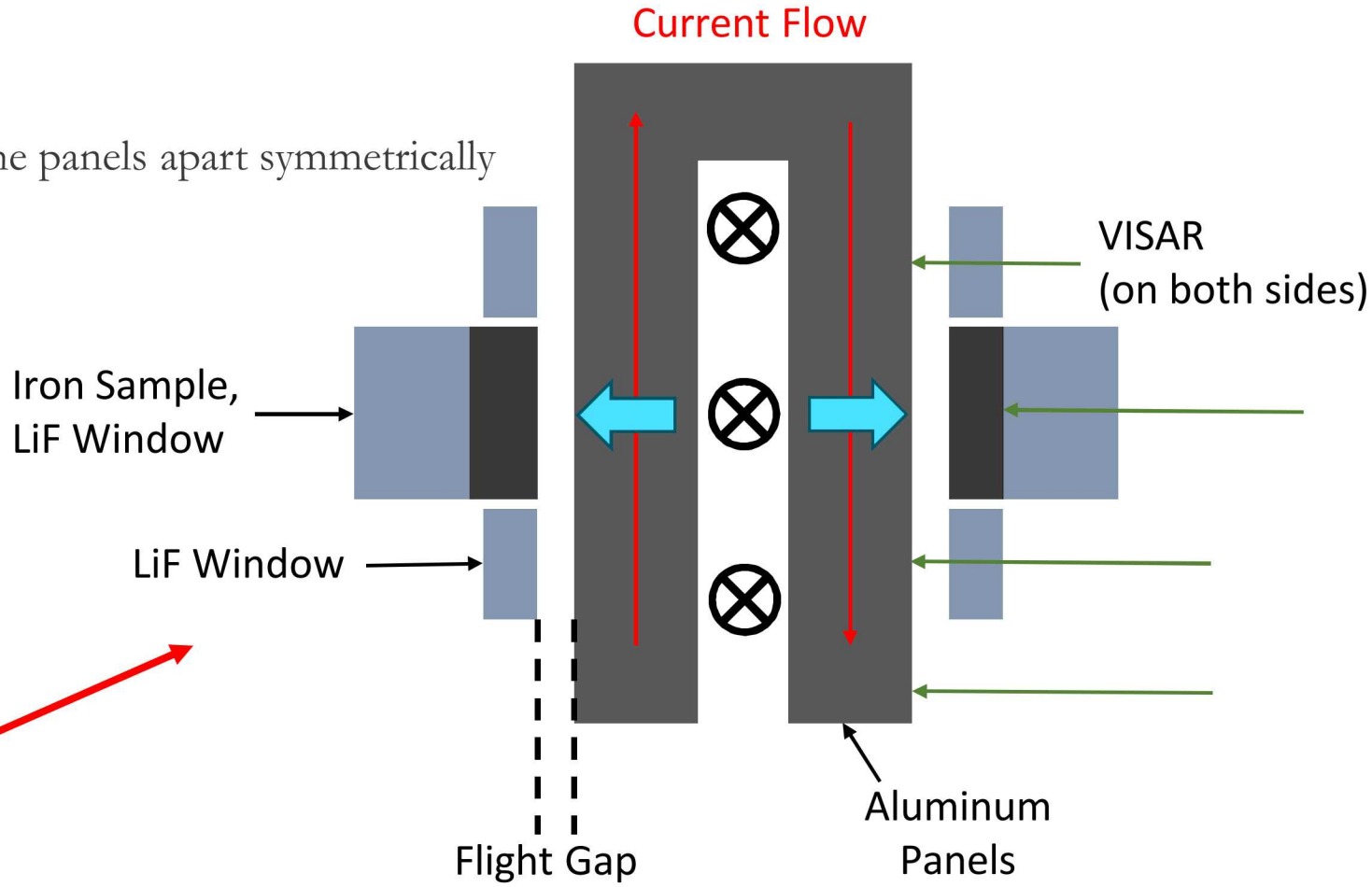

Conductivity Measurements with Ellipsometry

Ellipsometry uses a polarized laser to probe material dielectric properties at the laser wavelength

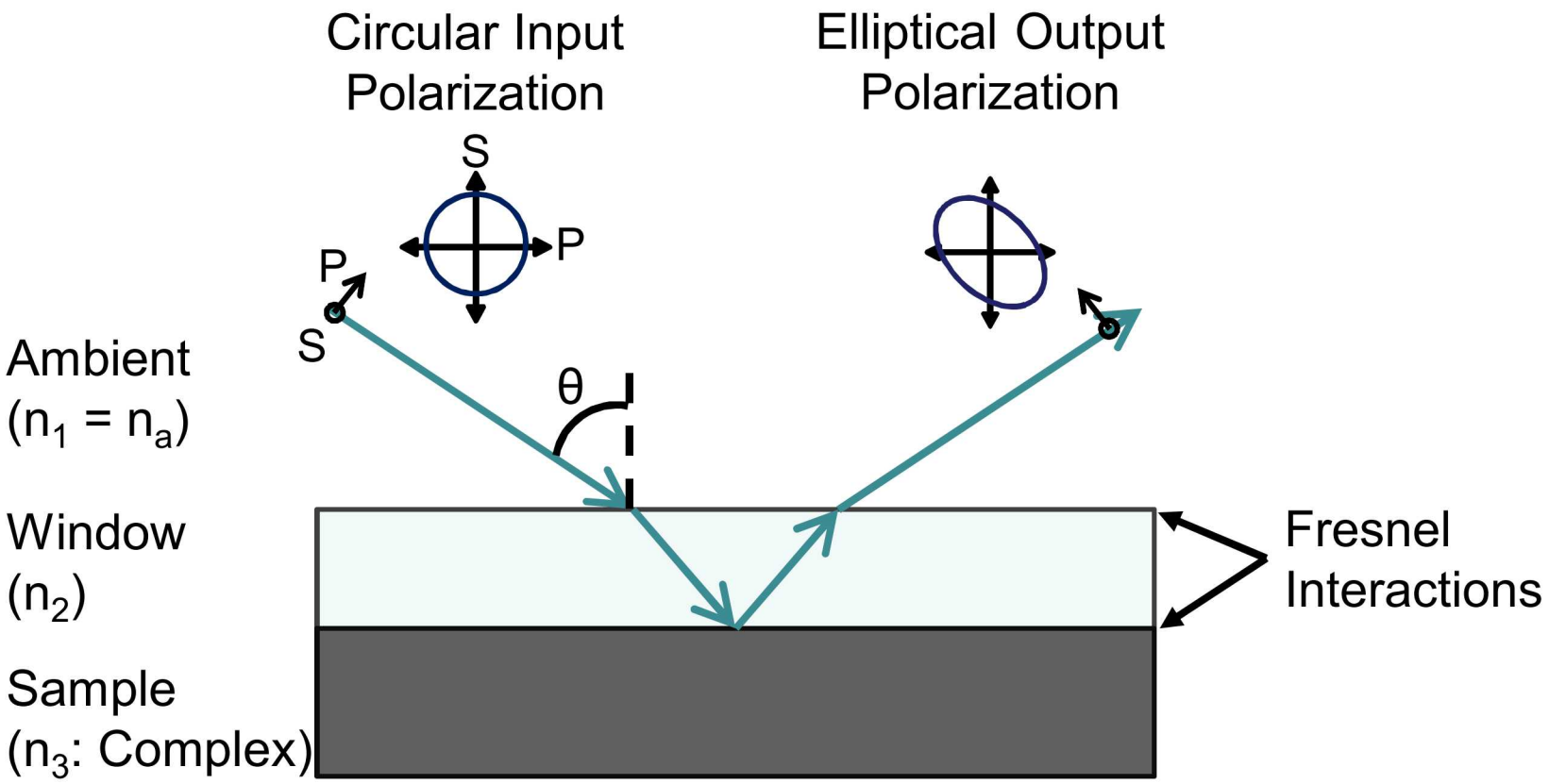

Along with the standard VISAR diagnostics, we have been fielding ellipsometry on one to two samples

Implementation of New Diagnostic

- Hardware/Procedural Changes
- No negative impact on other diagnostics or experiment

Advantages of this Experiment

- Overdriving detrimental window effects
- Minimal tilt compared to gas guns
- AC conductivity closely matches DC conductivity at these wavelengths

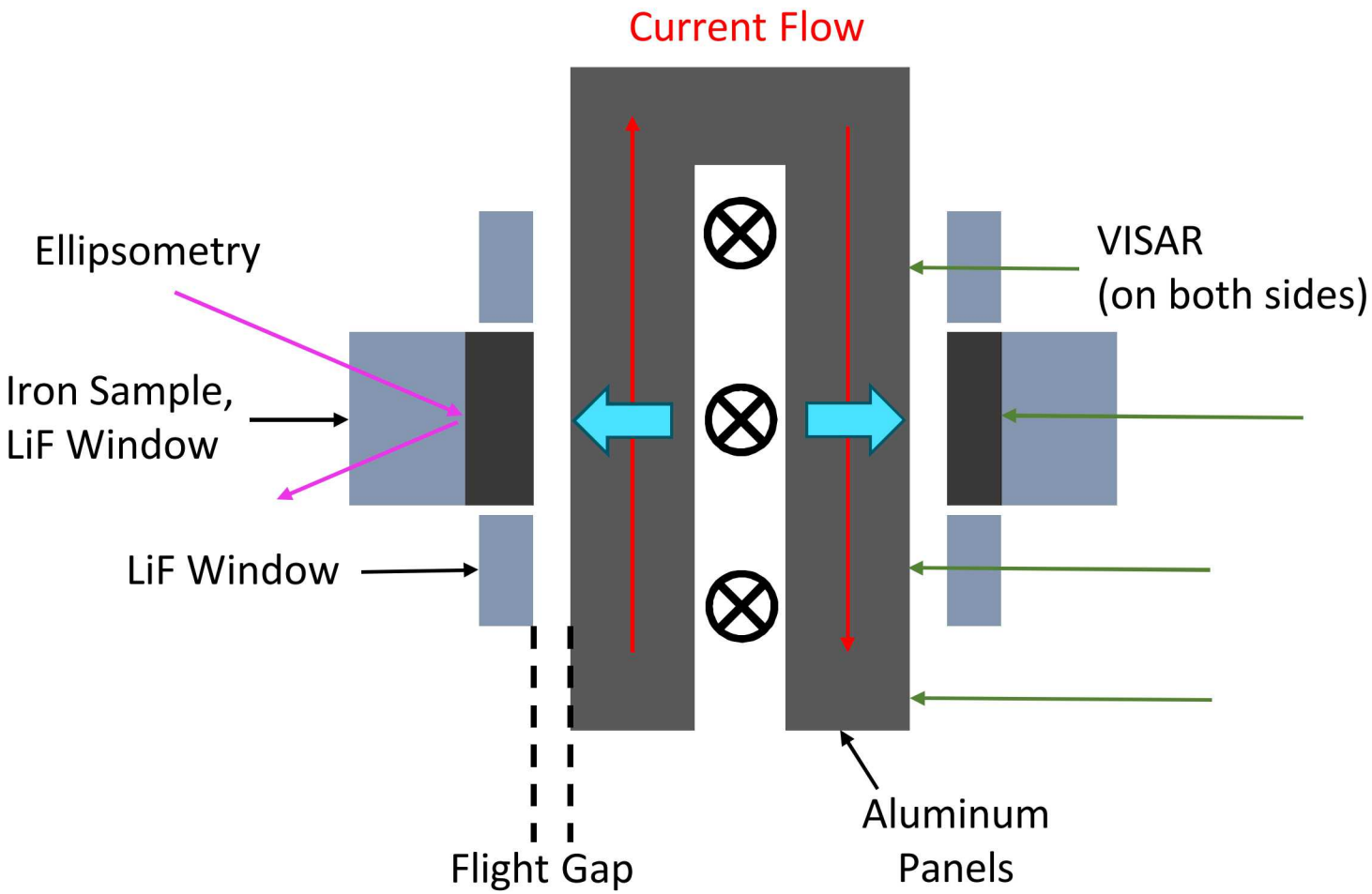

The Z hardware engineers made the fielding of this diagnostic possible

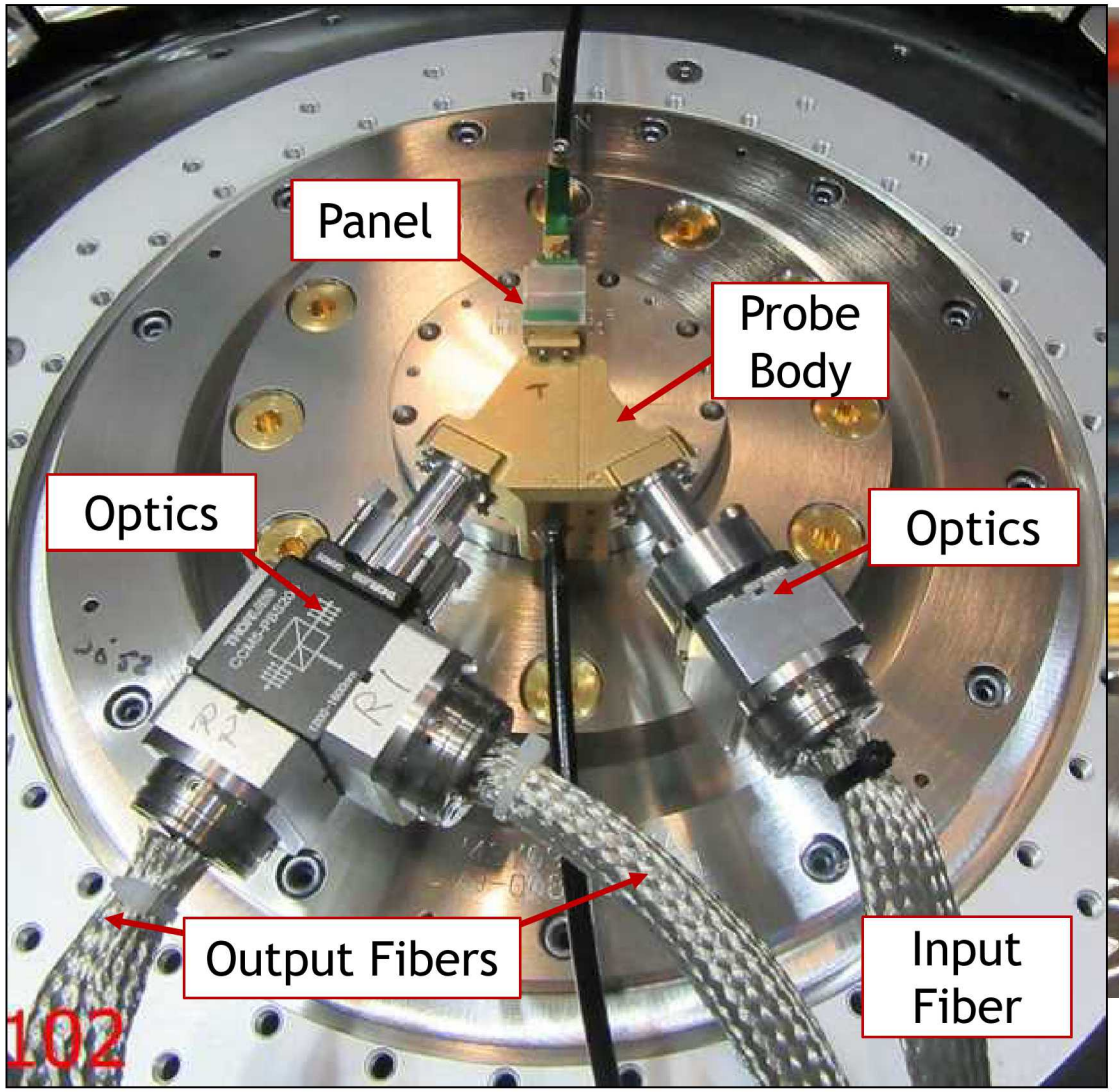

Obtaining specular reflections on dynamic experiments is difficult

Surface roughness and impactor tilt can severely hinder such measurements

- Surface roughness can be propagated through the shock wave

Ellipsometry depends on AOI

- cannot simply increase the collection

Ensure all surfaces are as smooth as possible

- Diamond turned metals (maybe lapping too)
  - 10-30 nm Ra
- Polished single crystal LiF
  - 20/10 scratch/dig

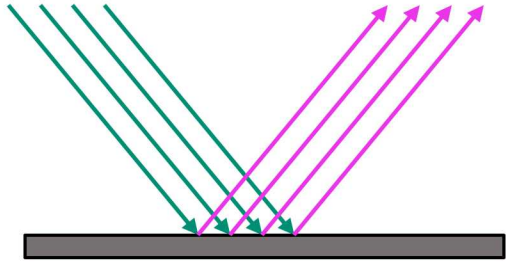

Specular Reflection

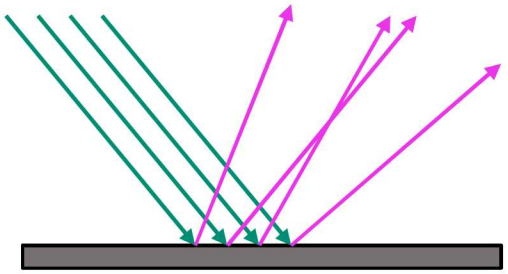

Scattered Reflection

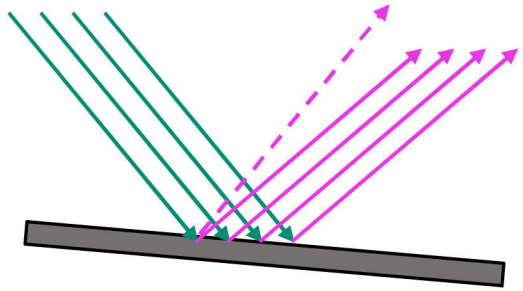

Tilted Reflection

Using a polished LiF 'sample' we obtained our best collection yet

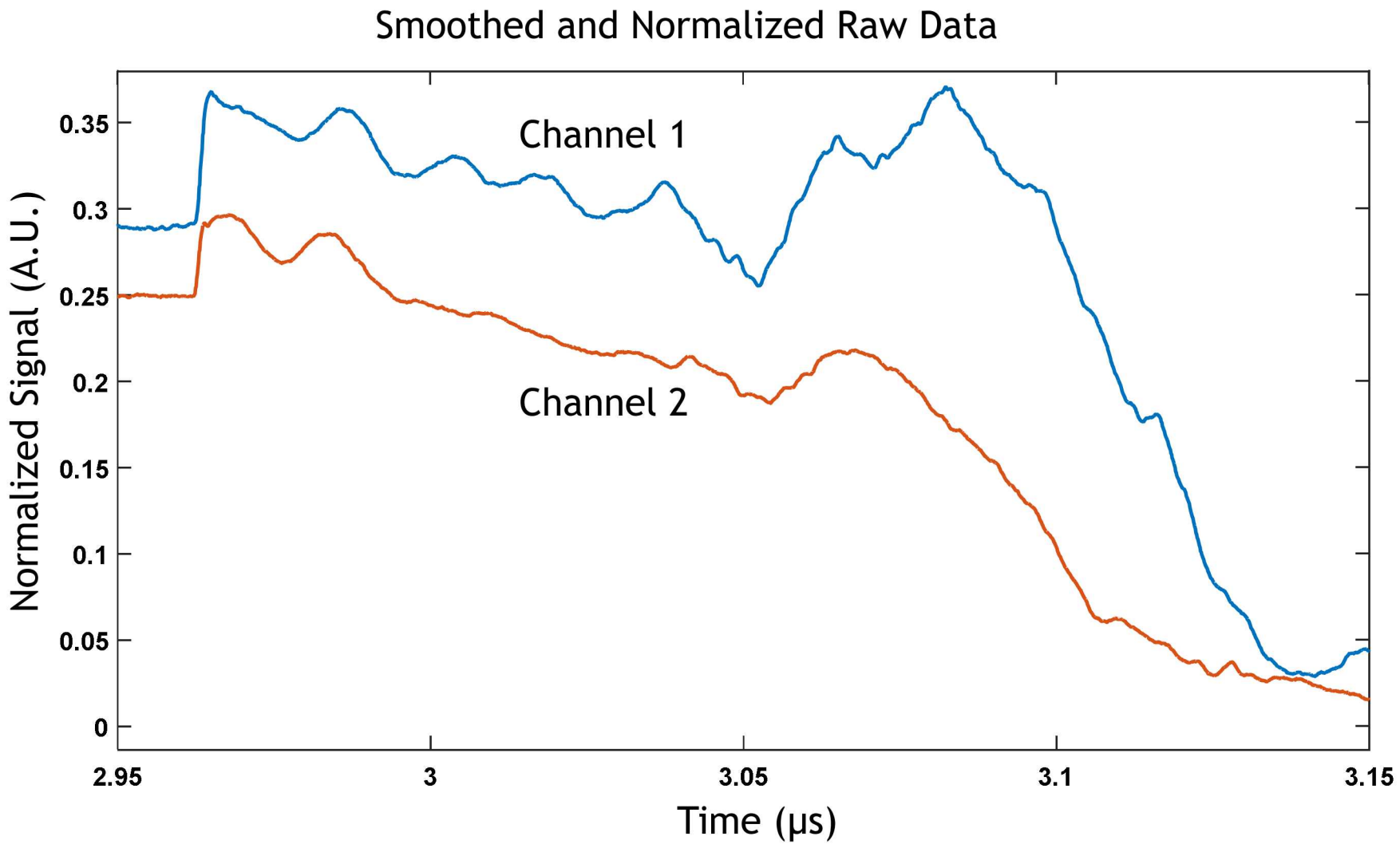

With increased focused on polishing, we were also able to see significant improvement on with an iron sample, though not as much as for the LiF sample arrangement

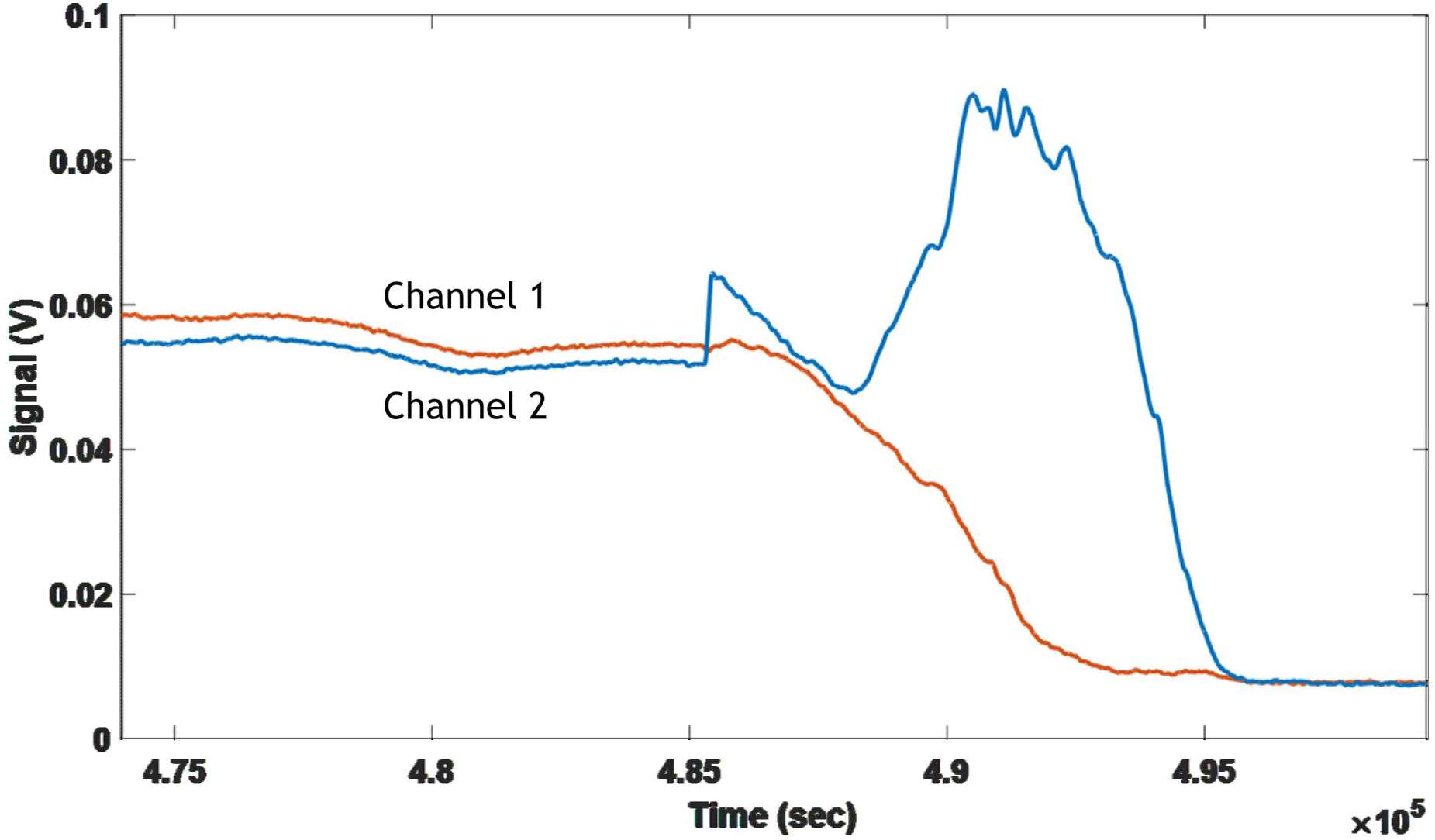

We can also use this diagnostic to study the shock-induced birefringence in window anvils

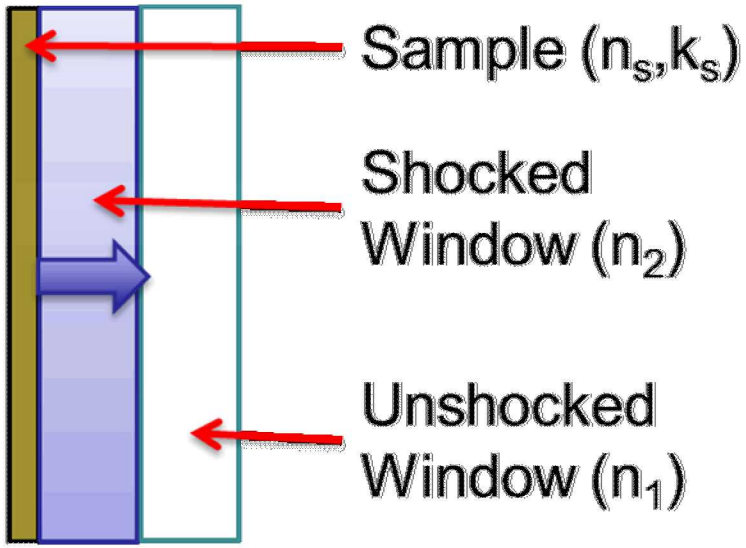

Shocked Index of Refraction:
$n_e = 1.5044 \pm 0.00005$
$n_o = 1.5007$ (ambient)

Ellipsometry Data and Model

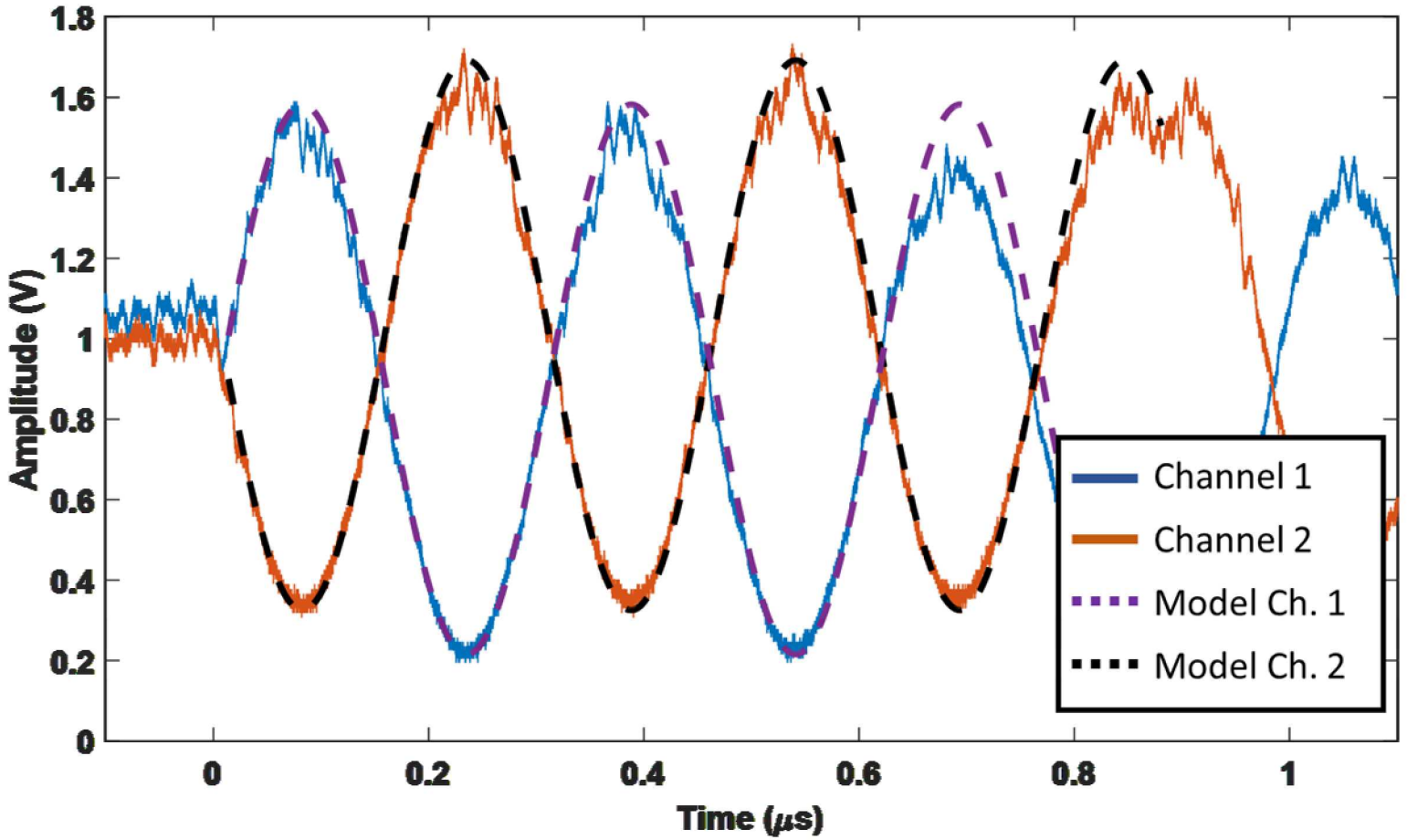

This can also be used to observe more complex wave structure

Simulated Release Profiles

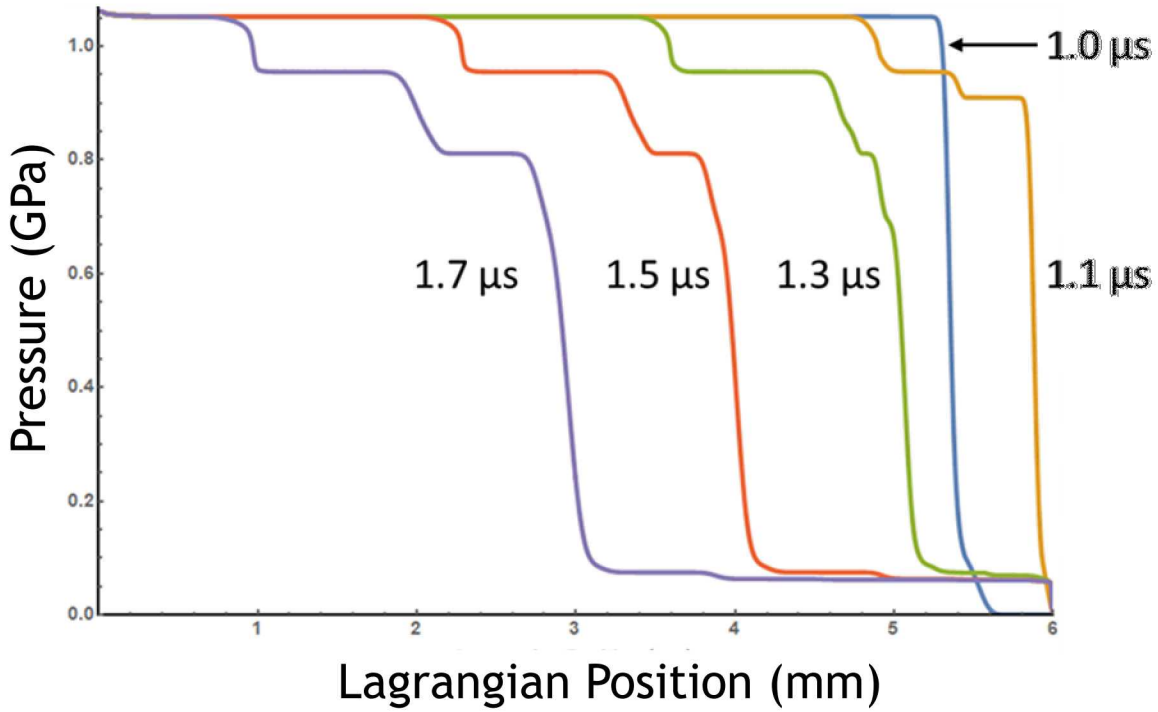

Ellipsometry Data

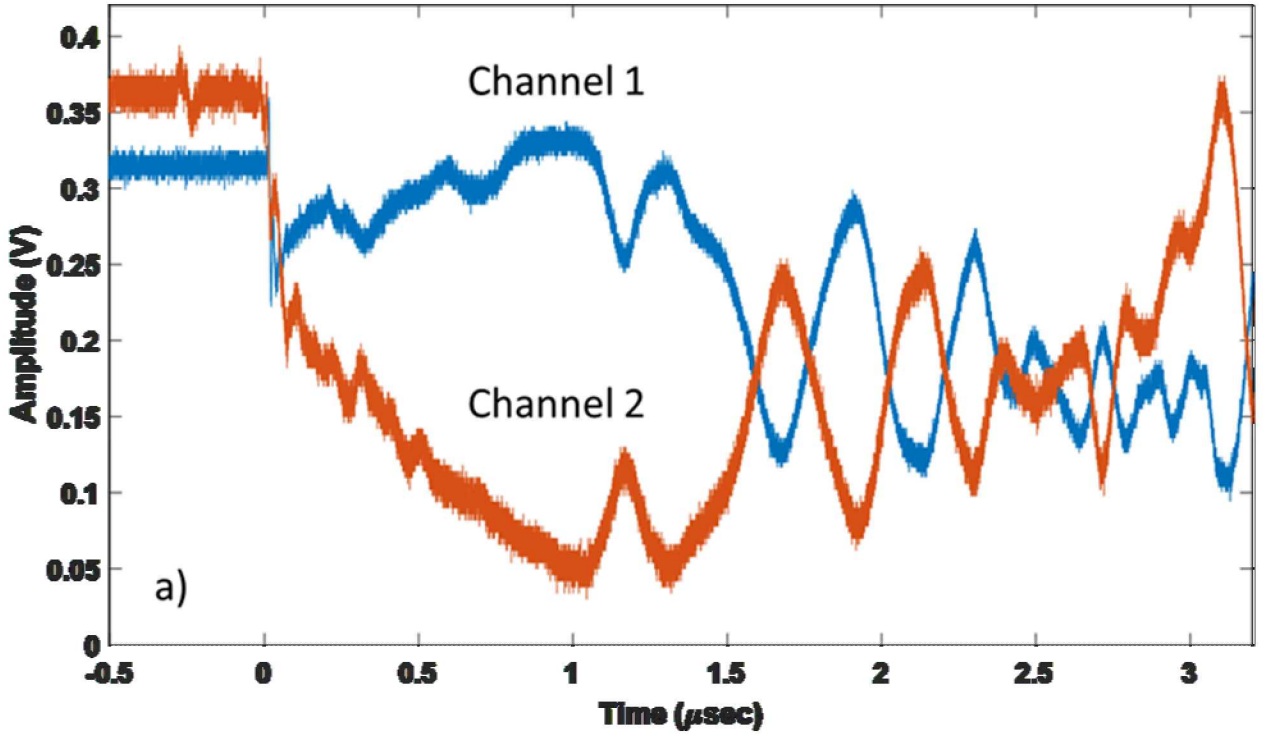

Equation of State

We use measurements of the particle velocity at all of the sample-window interfaces, provided by VISAR

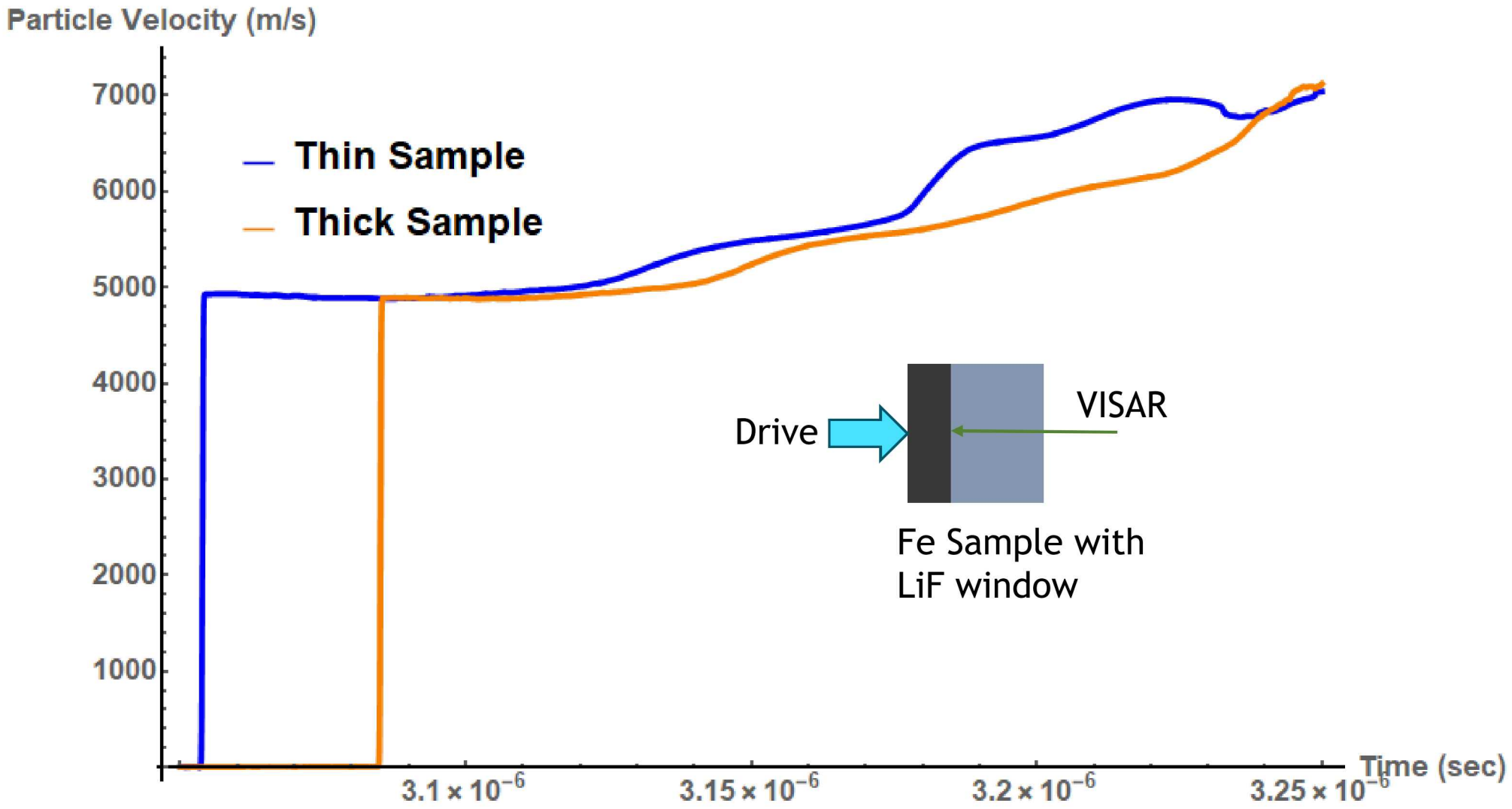

An iterative backward-integration forward Lagrangian analysis is used to build the equation of state

Backward Integration

- The Lagrangian hydrodynamic equations along with a guess of the equation of state are backward integrated to obtain the drive profile at the sample-impactor interface:

$$\frac{\delta[P(\rho)]}{\delta x} = -\rho_0 \frac{\delta u}{\delta t}$$

$$\frac{1}{\rho_0}\frac{\delta u}{\delta x} = \frac{\delta\left[\frac{1}{\rho}\right]}{\delta t}$$

Davis, J.-P. "Experimental measurement of the principal isentrope for aluminum 6061-T6 to 240 GPa." *Journal of applied physics* 99.10 (2006): 103512.

Seagle, C. T., and A. J. Porwitzky. "Shock-ramp compression of tin near the melt line." *AIP Conference Proceedings*. Vol. 1979. No. 1. AIP Publishing, 2018.

The drive conditions for the two samples should be equal until the release wave from the thin sample reaches this interface

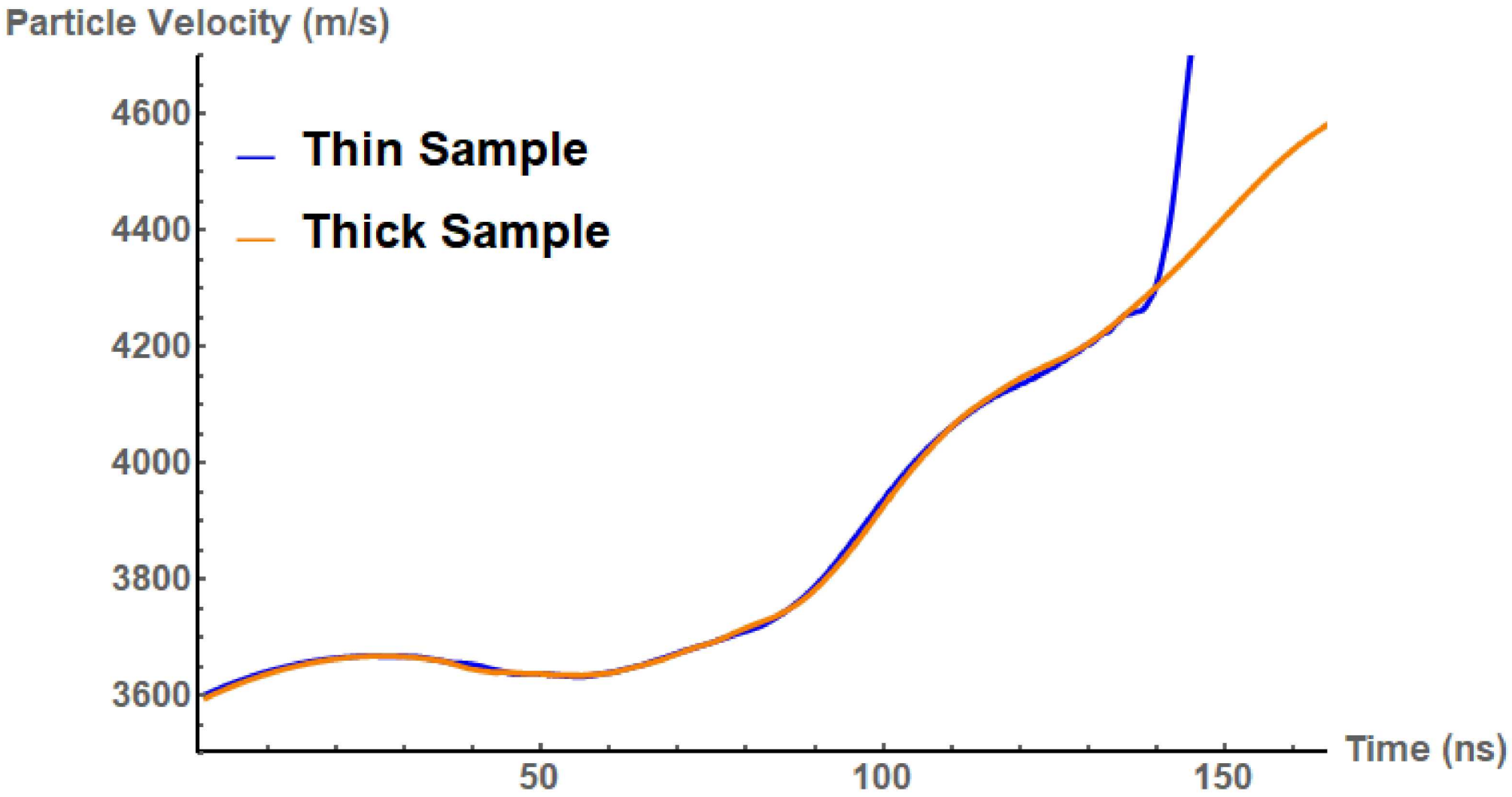

An iterative backward-integration forward Lagrangian analysis is used to build the equation of state

Backward Integration

- The Lagrangian hydrodynamic equations along with a guess of the equation of state are backward integrated to obtain the drive profile at the sample-impactor interface:

$$\frac{\delta[P(\rho)]}{\delta x} = -\rho_0 \frac{\delta u}{\delta t}$$

$$\frac{1}{\rho_0}\frac{\delta u}{\delta x} = \frac{\delta\left[\frac{1}{\rho}\right]}{\delta t}$$

Forward Propagation

- The drive state can then be propagated forward to the sample-window interface to obtain the *in-situ* particle velocity (the particle velocity that would have been present at that location had there not been a release interface)

The drive condition is propagated forward to the sample-window interface location

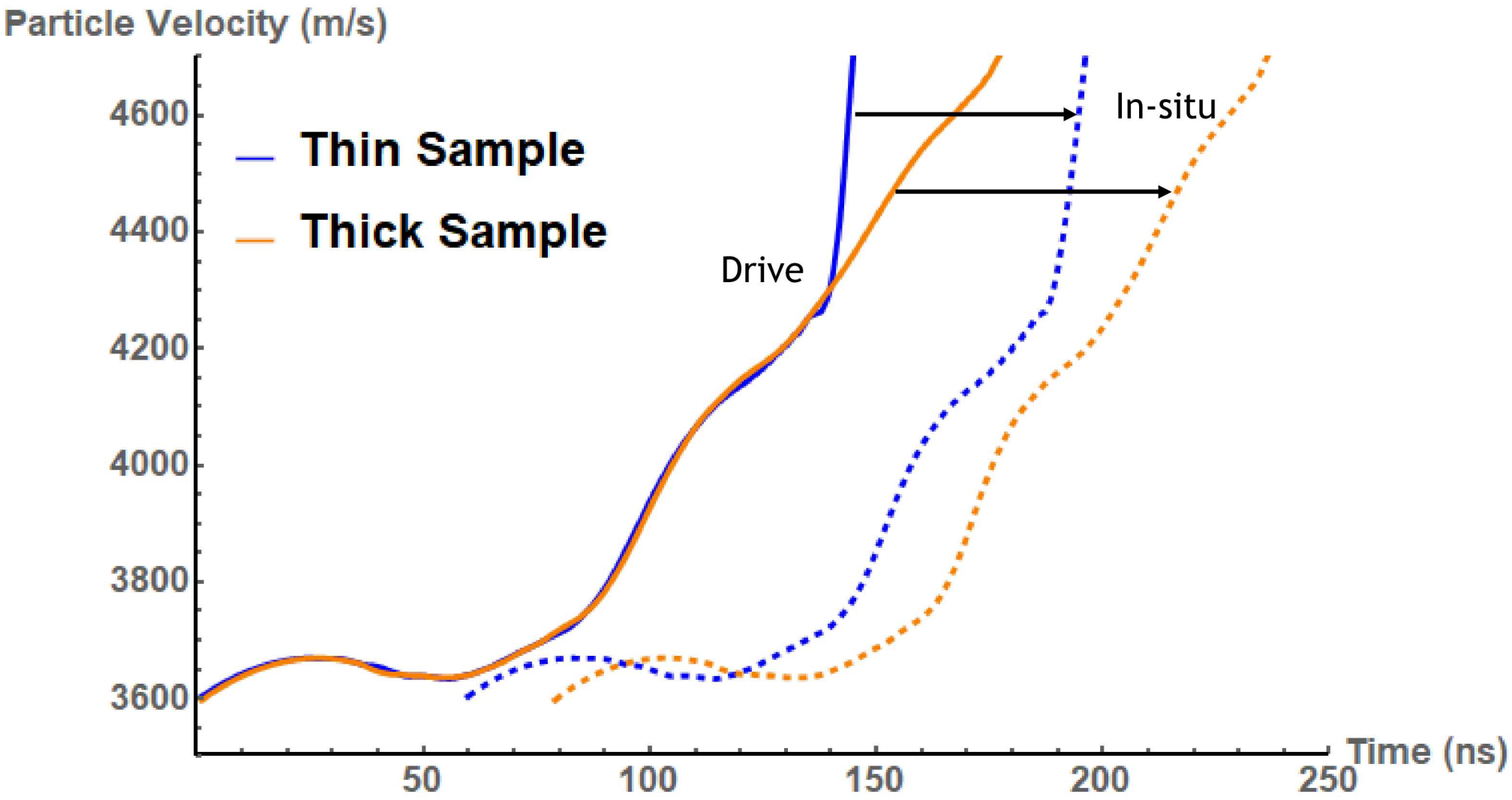

An iterative backward-integration forward Lagrangian analysis is used to build the equation of state

Backward Integration

- The Lagrangian hydrodynamic equations along with a guess of the equation of state are backward integrated to obtain the drive profile at the sample-impactor interface:

$$\frac{\delta[P(\rho)]}{\delta x} = -\rho_0 \frac{\delta u}{\delta t}$$

$$\frac{1}{\rho_0}\frac{\delta u}{\delta x} = \frac{\delta\left[\frac{1}{\rho}\right]}{\delta t}$$

Forward Propagation

- The drive state can then be propagated forward to the sample-window interface to obtain the *in-situ* particle velocity (the particle velocity that would have been present at that location had there not been a release interface)

Lagrangian Sound Speed and EOS

- A sound speed can then be directly calculated from $\Delta x/\Delta t$ measurements
- A P-ρ EOS is formed from the sound speed:

$$\frac{1}{\rho_f} = \frac{1}{\rho_s} - \int_{u_{ps}}^{u_{pf}} \frac{du_p}{\rho_0 C_L}$$

$$P_f = P_s + \int_{u_{ps}}^{u_{pf}} \rho_0 C_L du_p$$

Lagrangian sound speed is determined, and used to calculate the equation of state

Sound Speed

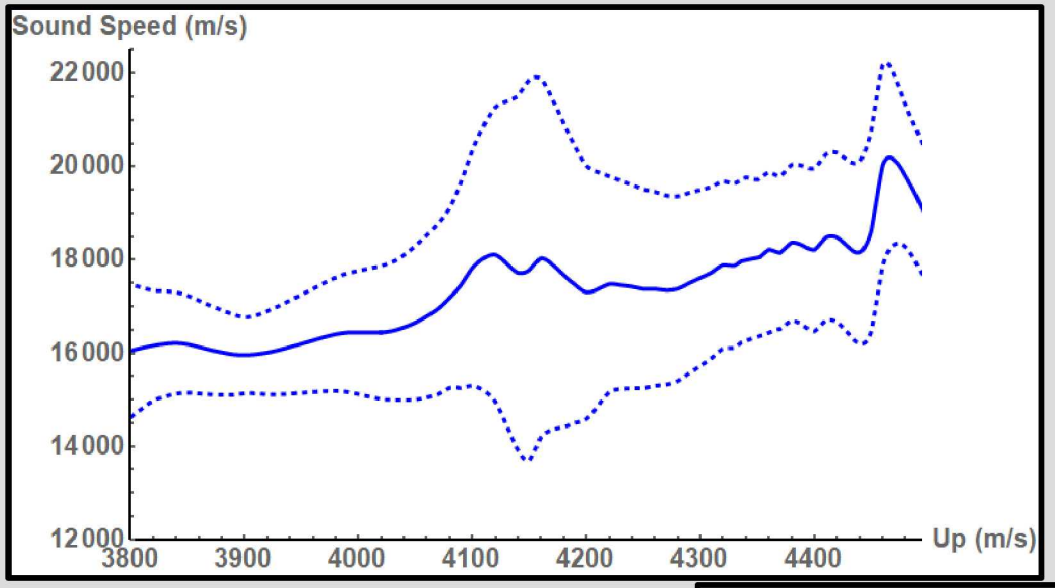

$$\frac{1}{\rho_f} = \frac{1}{\rho_s} - \int_{u_{ps}}^{u_{pf}} \frac{du_p}{\rho_0 C_L}$$

$$P_f = P_s + \int_{u_{ps}}^{u_{pf}} \rho_0 C_L du_p$$

Equation of State

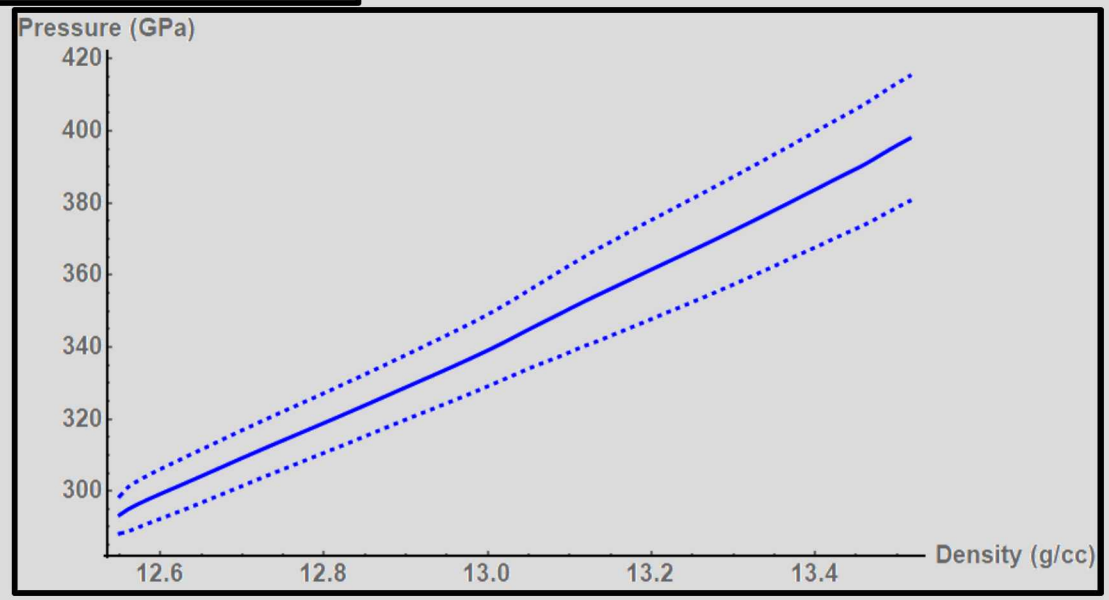

An iterative backward-integration forward Lagrangian analysis is used to build the equation of state

Backward Integration

- The Lagrangian hydrodynamic equations along with a guess of the equation of state are backward integrated to obtain the drive profile at the sample-impactor interface:

$$\frac{\delta[P(\rho)]}{\delta x} = -\rho_0 \frac{\delta u}{\delta t}$$

$$\frac{1}{\rho_0}\frac{\delta u}{\delta x} = \frac{\delta\left[\frac{1}{\rho}\right]}{\delta t}$$

Forward Propagation

- The drive state can then be propagated forward to the sample-window interface to obtain the *in-situ* particle velocity (the particle velocity that would have been present at that location had there not been a release interface)

Lagrangian Sound Speed and EOS

- A sound speed can then be directly calculated from $\Delta x/\Delta t$ measurements
- A P-ρ EOS is formed from the sound speed:

$$\frac{1}{\rho_f} = \frac{1}{\rho_s} - \int_{u_{ps}}^{u_{pf}} \frac{du_p}{\rho_0 C_L}$$

$$P_f = P_s + \int_{u_{ps}}^{u_{pf}} \rho_0 C_L du_p$$

Iterate

- The process is then repeated with this new EOS
- This iterative process continues until the new EOS matches the solution from the previous iteration

An iterative backward-integration forward Lagrangian analysis is used to build the equation of state

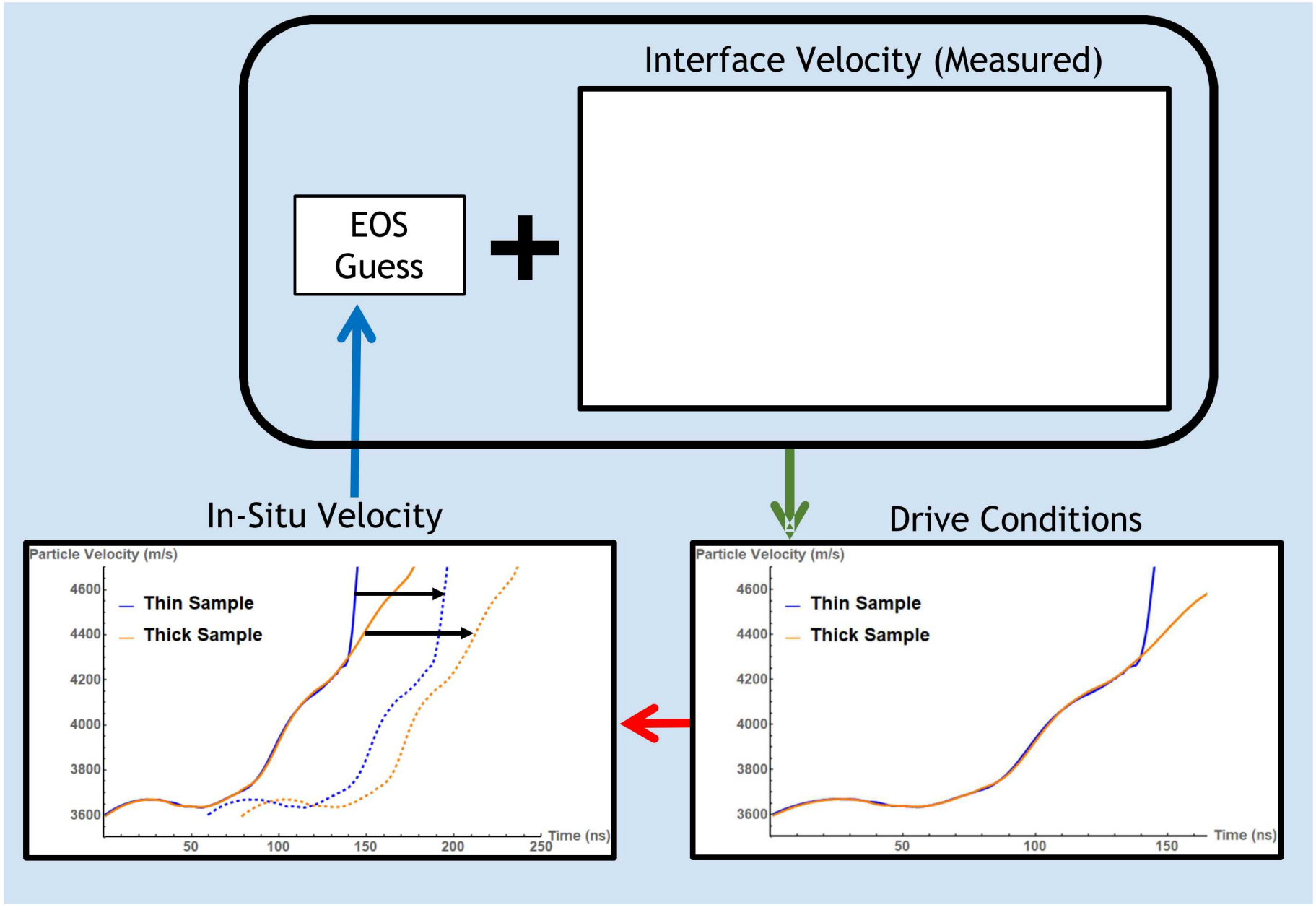

Results from our previous experiment agree well with current EOS tables

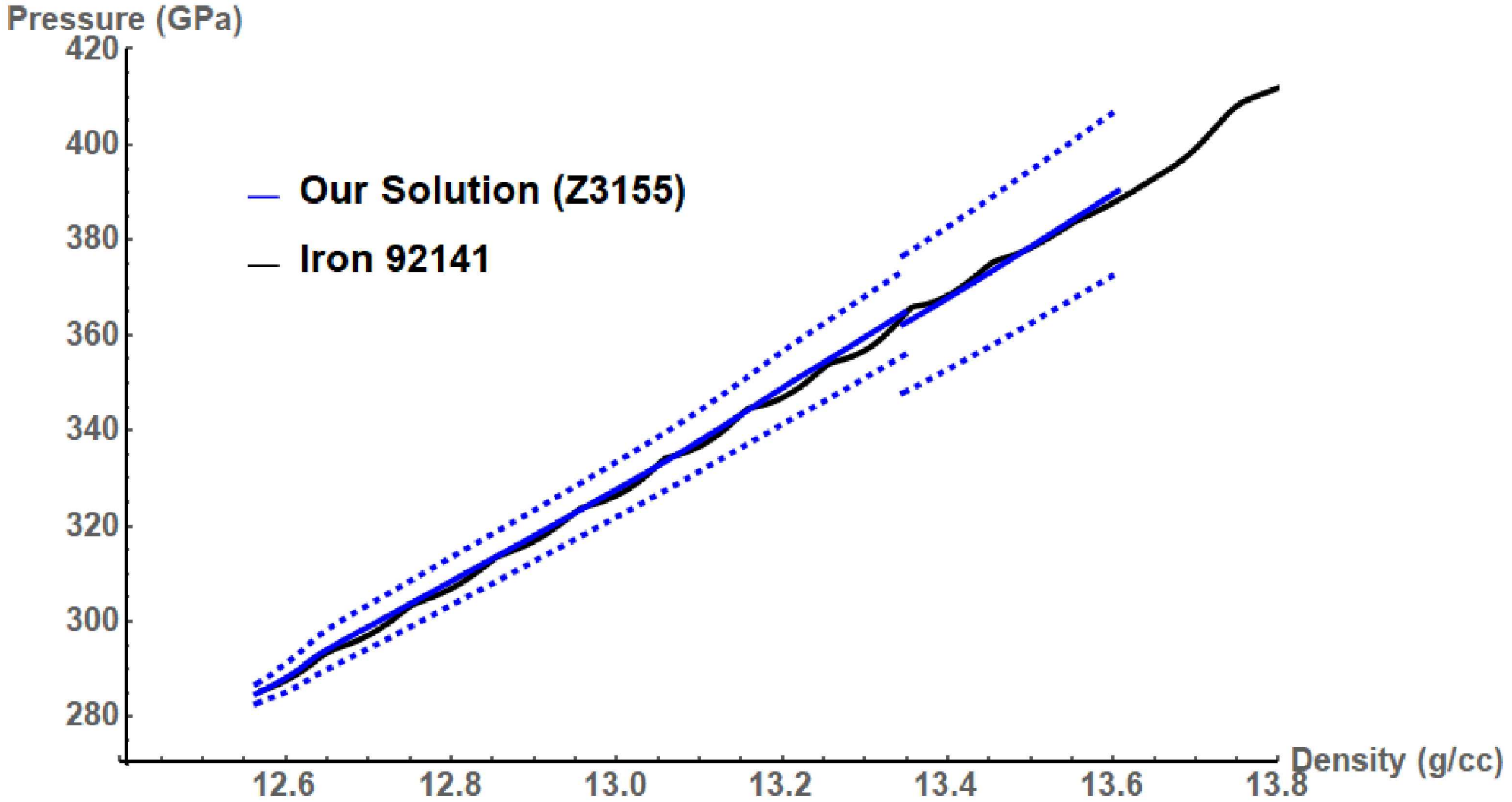

Sjostrom, T., & Crockett, S. (2018). Quantum molecular dynamics of warm dense iron and a five-phase equation of state. Physical Review E, 97(5), 053209.

This framework typically assumes a steady shock front before the ramp

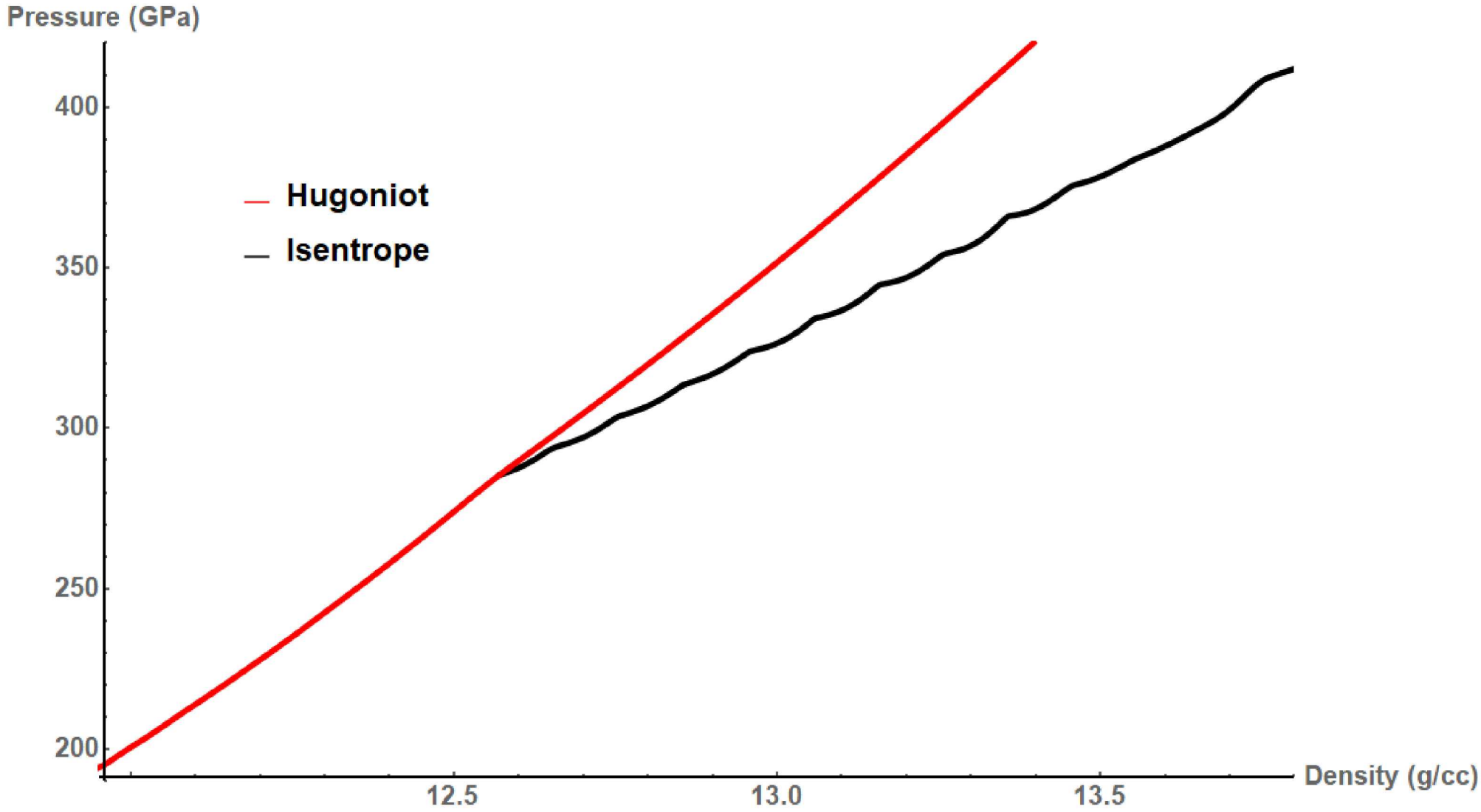

This framework typically assumes a steady shock front before the ramp

- Our most recent experiment experienced noticeable decay on the initial shock state

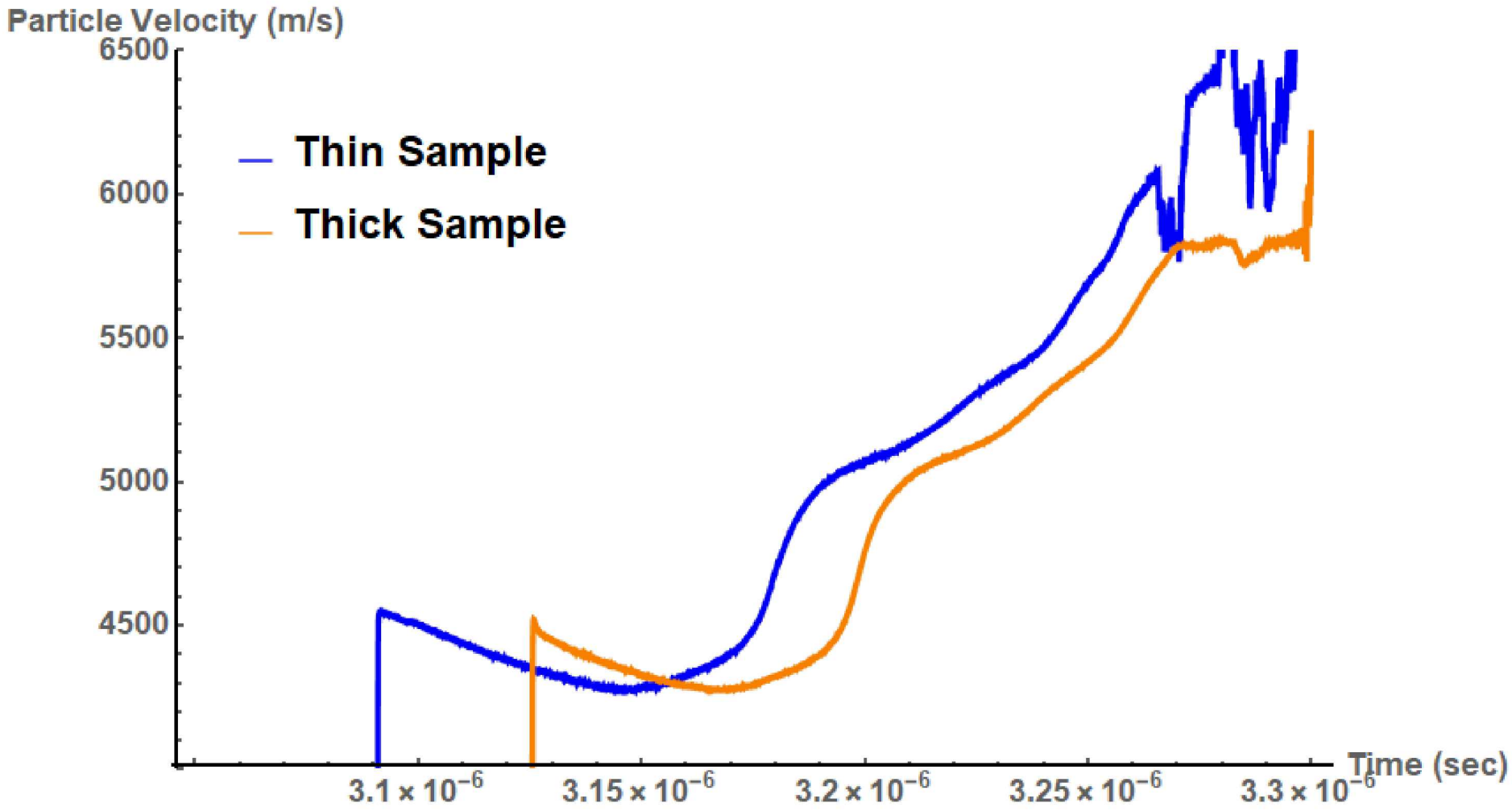

The experiment is no longer constrained along a single isentrope

- Instead, a range of isentropes are covered based on the Lagrangian position of the sample

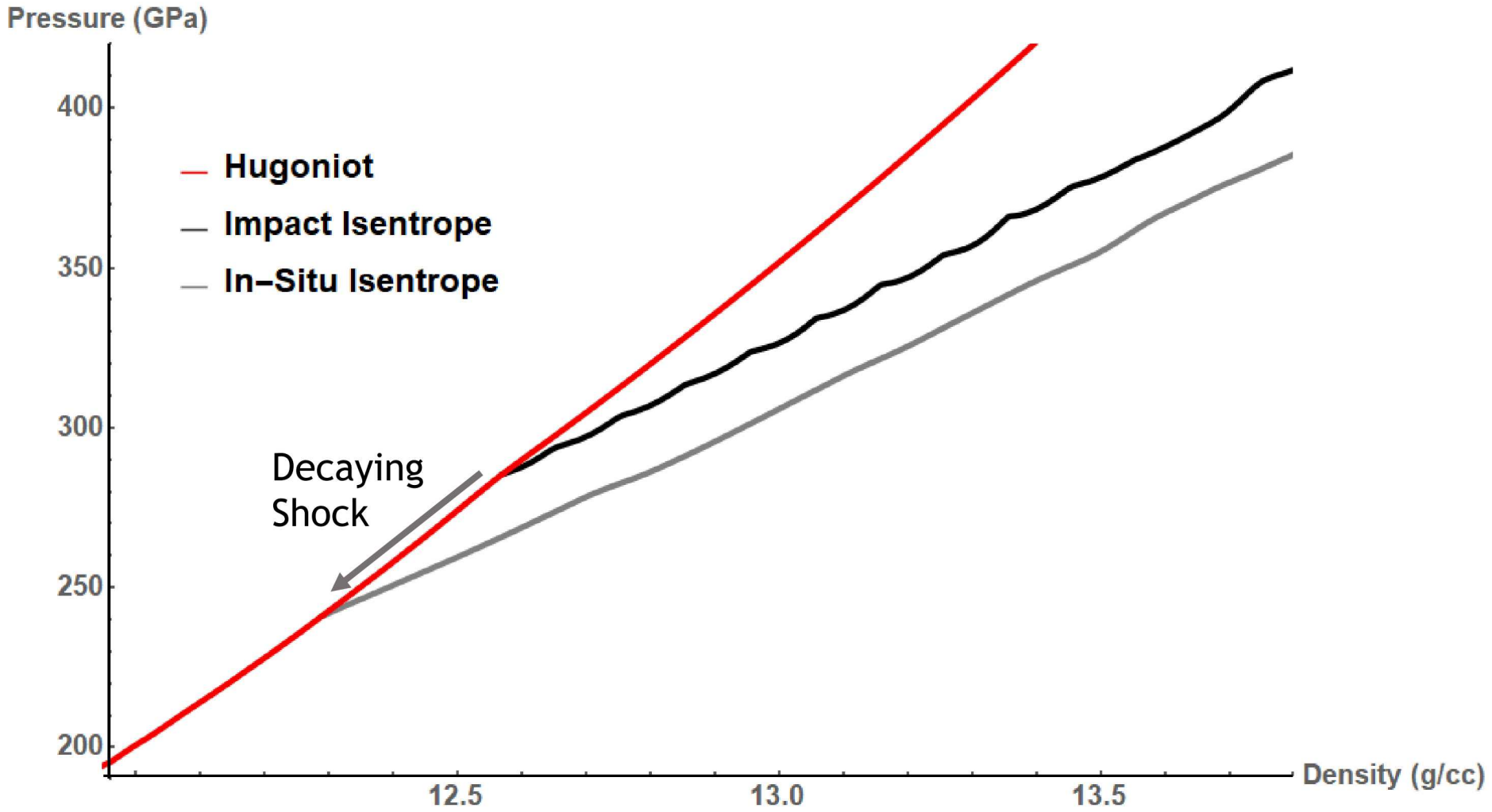

With modifications to the standard analysis, we analyzed the data from the three sample pairs in Z3339

Modifications primarily include:

- The shock-front, and associated boundary condition, varies as a function of Lagrangian position, based on the observed shock states at impact and the two sample-window interfaces.
- Instead of inputting a single isentrope EOS as the 'guess' into the iterative process, a range of isentropes covering the conditions defined by the variable shock state must be provided or generated by the user.

With modifications to the standard analysis, we analyzed the data from the three sample pairs in Z3339

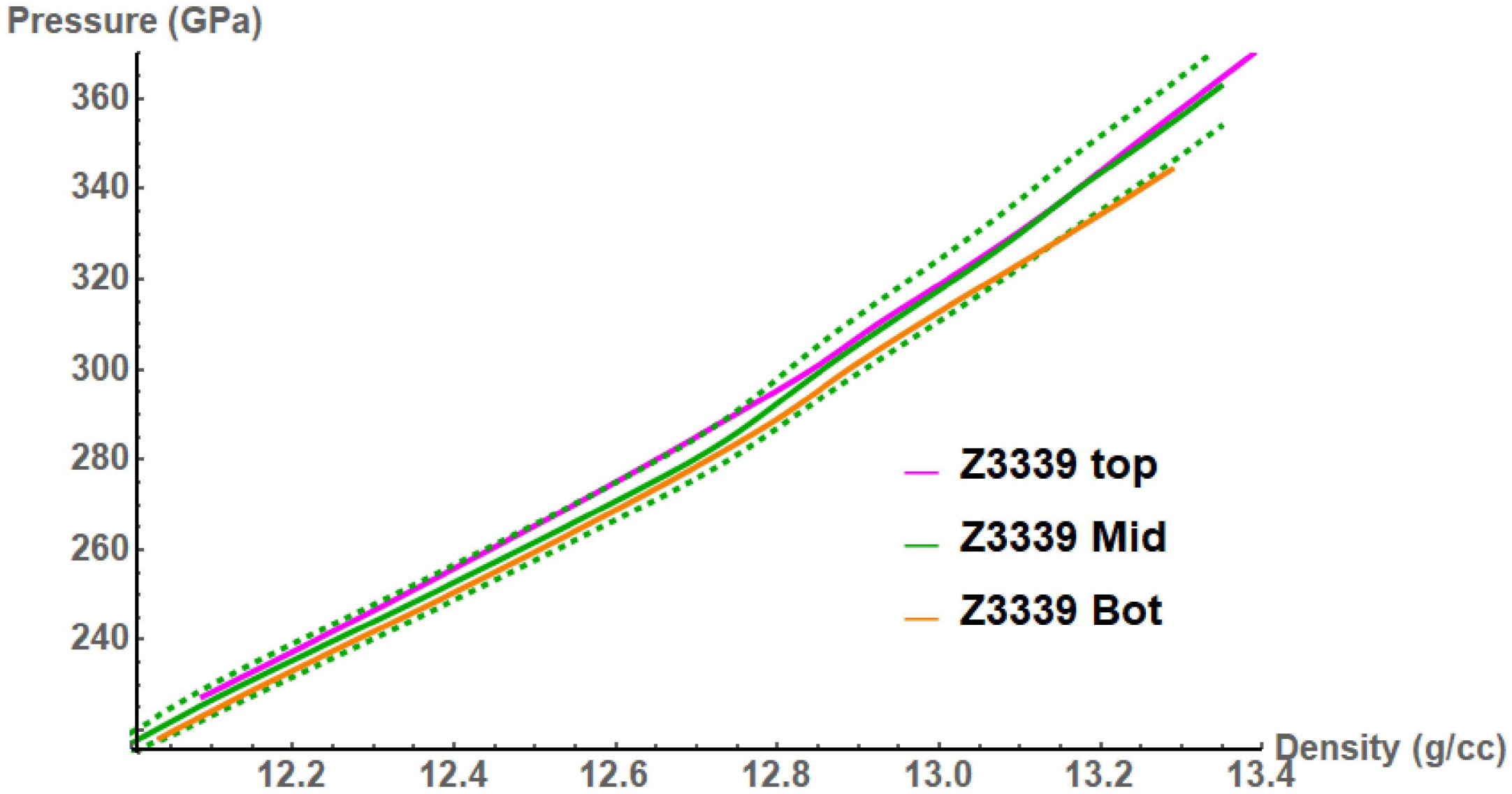

However, the latter half of these data sets are not adequately converging

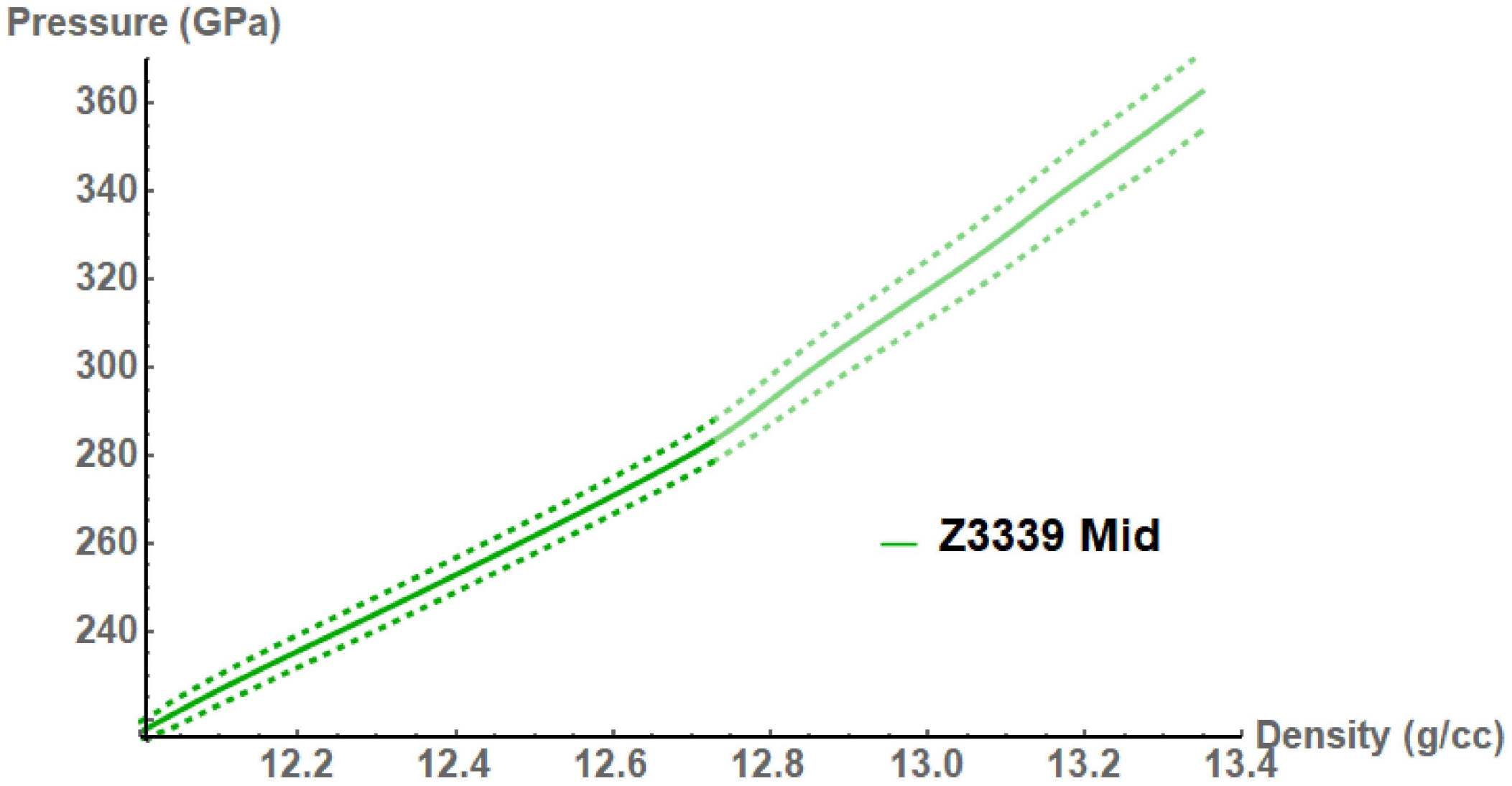

We combine the relevant data from all three sample pairs

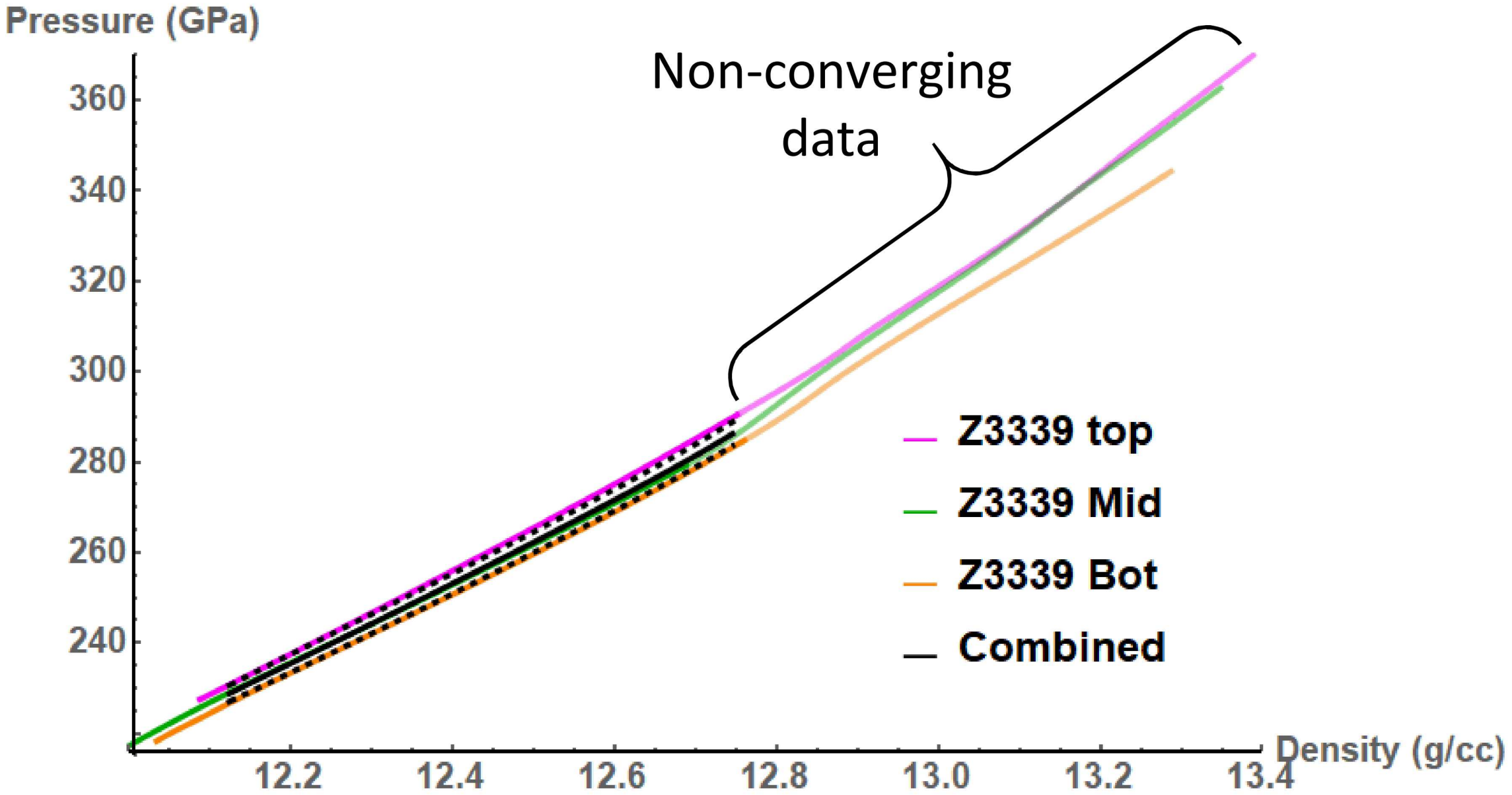

Our two data sets both agree well with the iron 92141 sesame EOS table

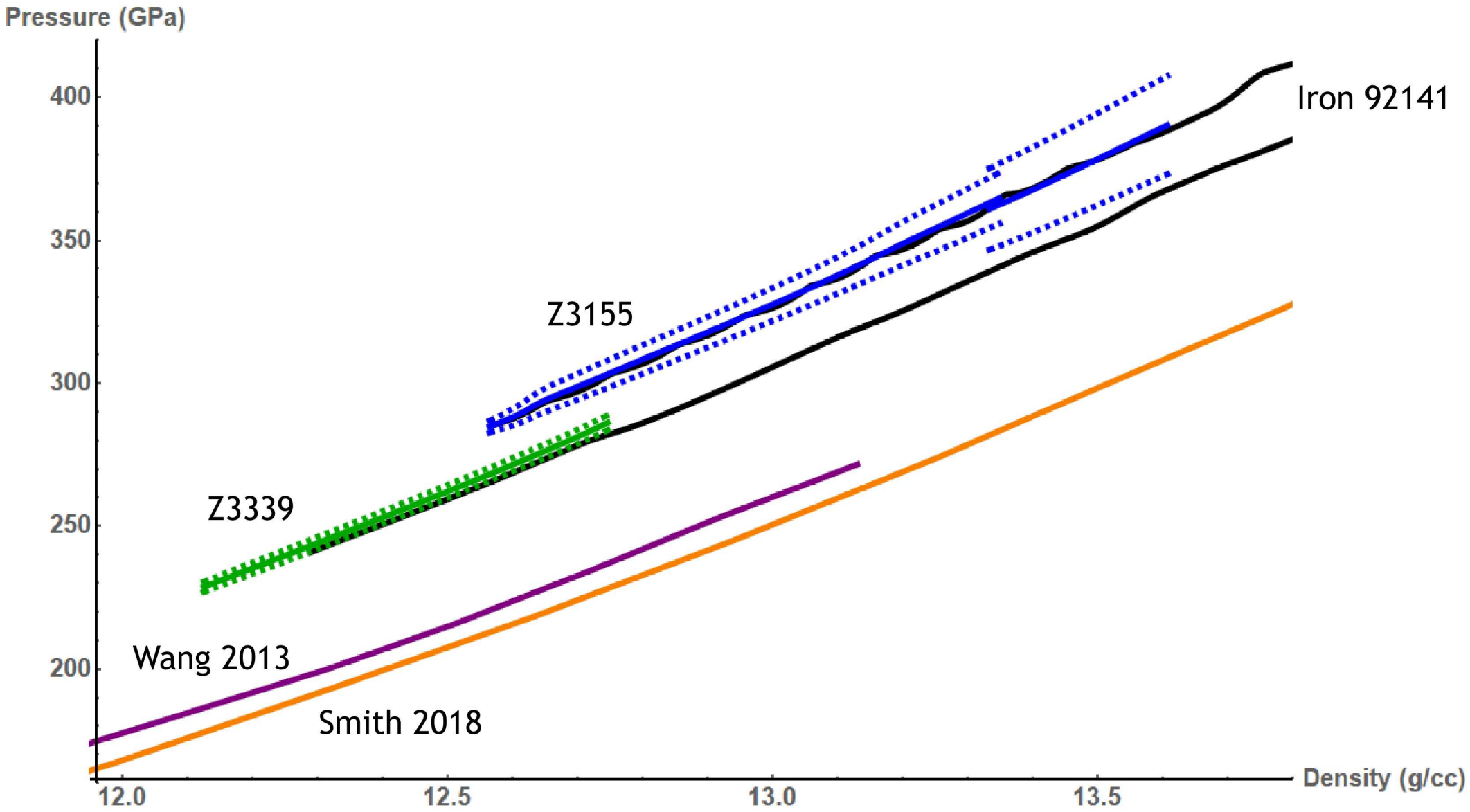

Equation of state information is often incorporated into research via parameters to analytic models

- Various analytic models
  - Birch-Murnaghan, Vinet, Mie-Gruneisen, etc.
- Planetary modeling codes
  - BurnMan
- Fit parameters for the existing liquid data: our results and previous shock data

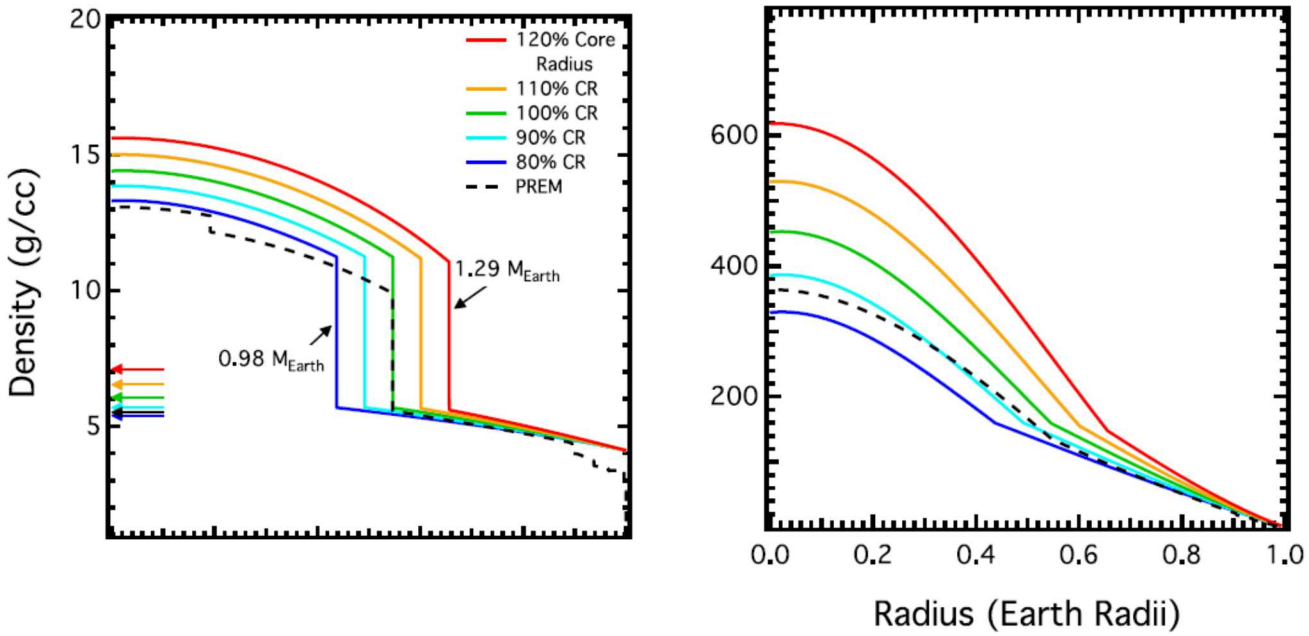

Figure 2. Density and pressure profiles for a two-layer (pure liquid Fe core and $MgSiO_3$-bridgmanite mantle) one $R_\oplus$ planet as a function of planetary radius for a variable core radius. PREM is shown in the black-dashed line for comparison. Average planet densities for each model are shown as arrows of same color scheme as density/pressure profiles. Figures 2–5 are all plotted on the same scale for comparison.

Unterborn, C. T., Dismukes, E. E., & Panero, W. R. (2016). Scaling the Earth: a sensitivity analysis of terrestrial exoplanetary interior models. The Astrophysical Journal, 819(1), 32.

We create a parameterized EOS model using the Ichikawa model to constrain some of the parameters

- Model:

$$P(\rho,T) = P_{iso}(\rho) + P_{th}(\rho,T)$$

$$P_{iso}(\rho) = 3\,K_0 \left(\frac{\rho}{\rho_0}\right)^{\frac{2}{3}} \left(1-\left(\frac{\rho_0}{\rho}\right)^{\frac{1}{3}}\right) Exp\left[\frac{3}{2}(K_0'-1)\left(1-\left(\frac{\rho_0}{\rho}\right)^{\frac{1}{3}}\right)\right]$$

$$P_{th}(\rho,T) = 3nR\,\gamma(\rho)\,\rho\left[(T-T_0) + e_0\left(\frac{\rho_0}{\rho}\right)^{g}(T^2-T_0^2)\right]$$

$$\gamma(\rho) = \gamma_0\left[1 + a\left(\left(\frac{\rho_0}{\rho}\right)^{b} - 1\right)\right]$$

Parameter	Ichikawa Values	Fit Values
K_0 (GPa)	24.6 ± 0.6	29.4 ± 3.7
K_0'	6.65 ± 0.04	6.21 ± 0.26
ρ_0 (g/cc)	5.187	
γ_0	1.85 ± 0.2	2.42 ± 0.09
a	1	
b	0.35	
e_0 (10^{-4}/K)	0.314	
g	-0.4	

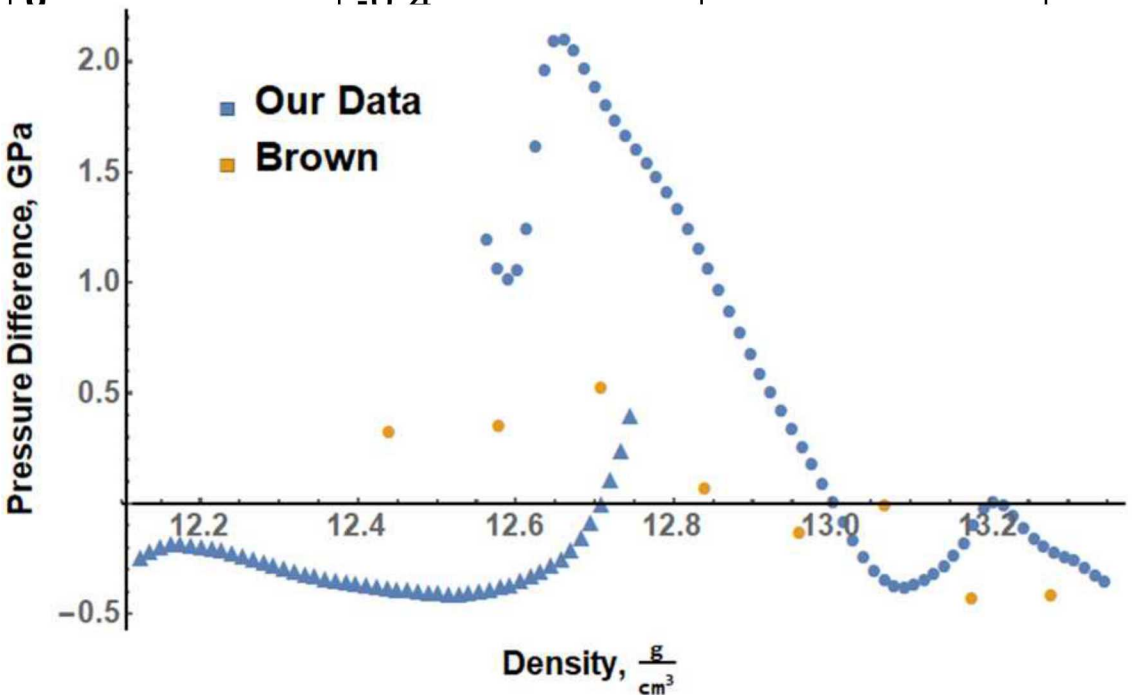

Can we use this to help infer the structure of newly discovered planets?

- The Kepler satellite detected over 2500 exoplanets
- The TESS satellite is currently discovering near-Earth-size planets

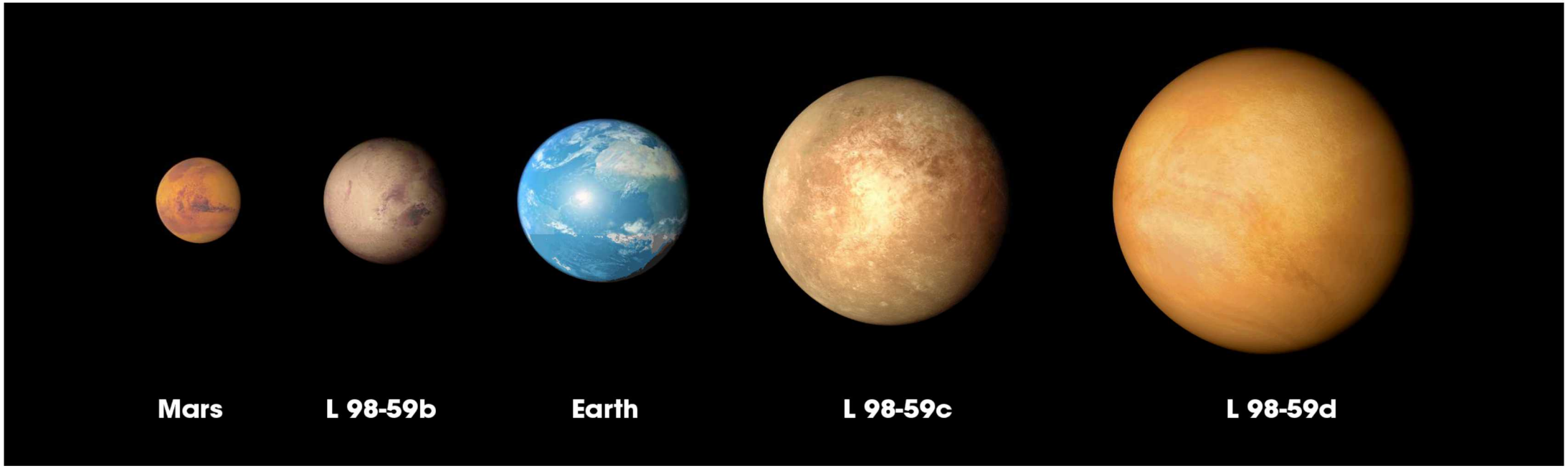

NASA's Goddard Space Flight Center
https://svs.gsfc.nasa.gov/13223

We model the radial structure of planets using the SESAME 92141 EOS for the core

- Model equations:

$$\frac{dm}{dr} = 4\pi r^2 \rho$$

$$\frac{dP}{dr} = -\frac{\rho\, G\, m(r)}{r^2}$$

$$\rho(r) = \rho_{eos}(P(r), T)$$

$$\frac{dT}{dr} = -\frac{\alpha\big(T(r)\big)\frac{Gm(r)}{r^2}T(r)}{C_P}$$

- Core EOS: Sesame 92141
- Mantle EOS: Katsura, 2010

1.2 Earth Mass Planet

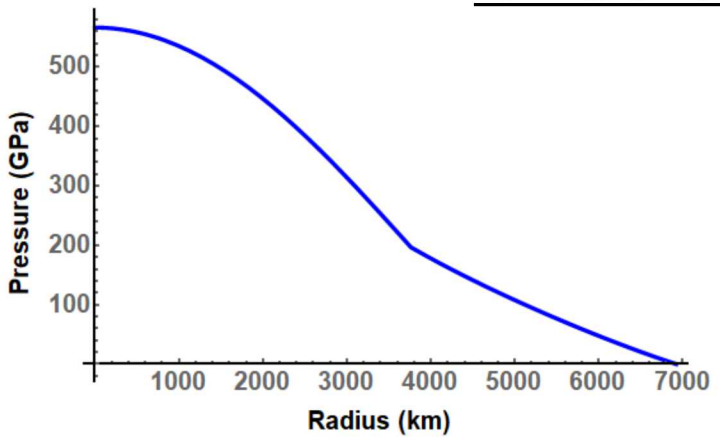

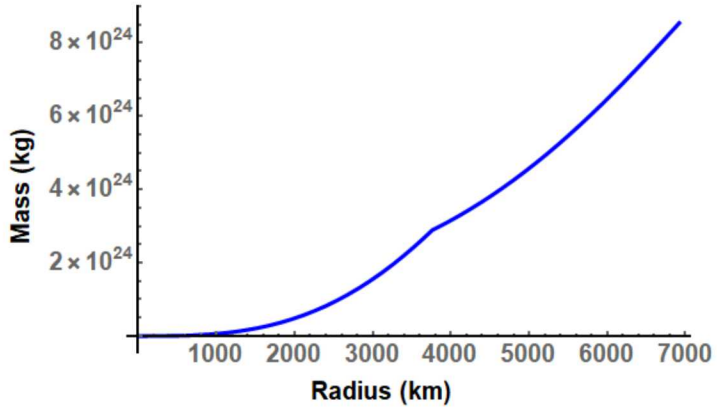

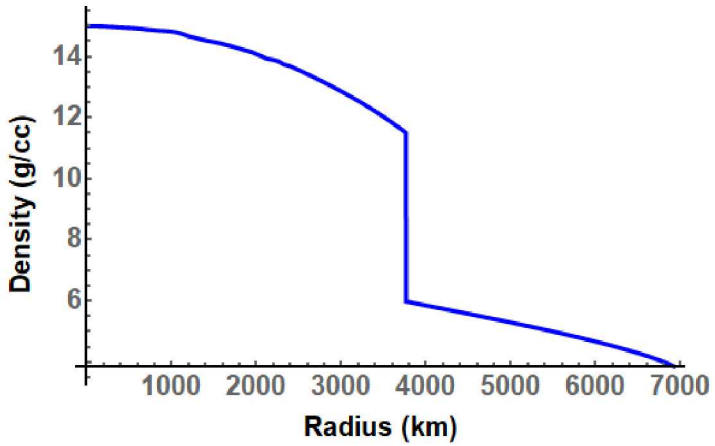

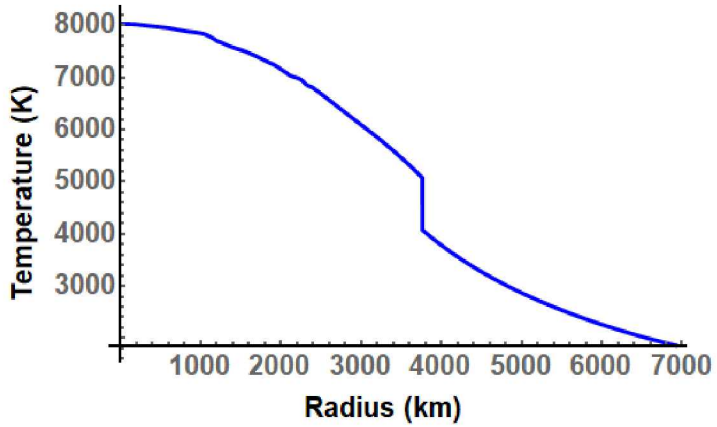

The mass-radius curves from the model informs planetary composition, and the models also reveal core structure

- M-R curves inform us about the composition of planets
- Our results are in close agreement with existing models
- Structural insight:
  - Liquid outer core only exists for planets up to 3.1 Earth masses

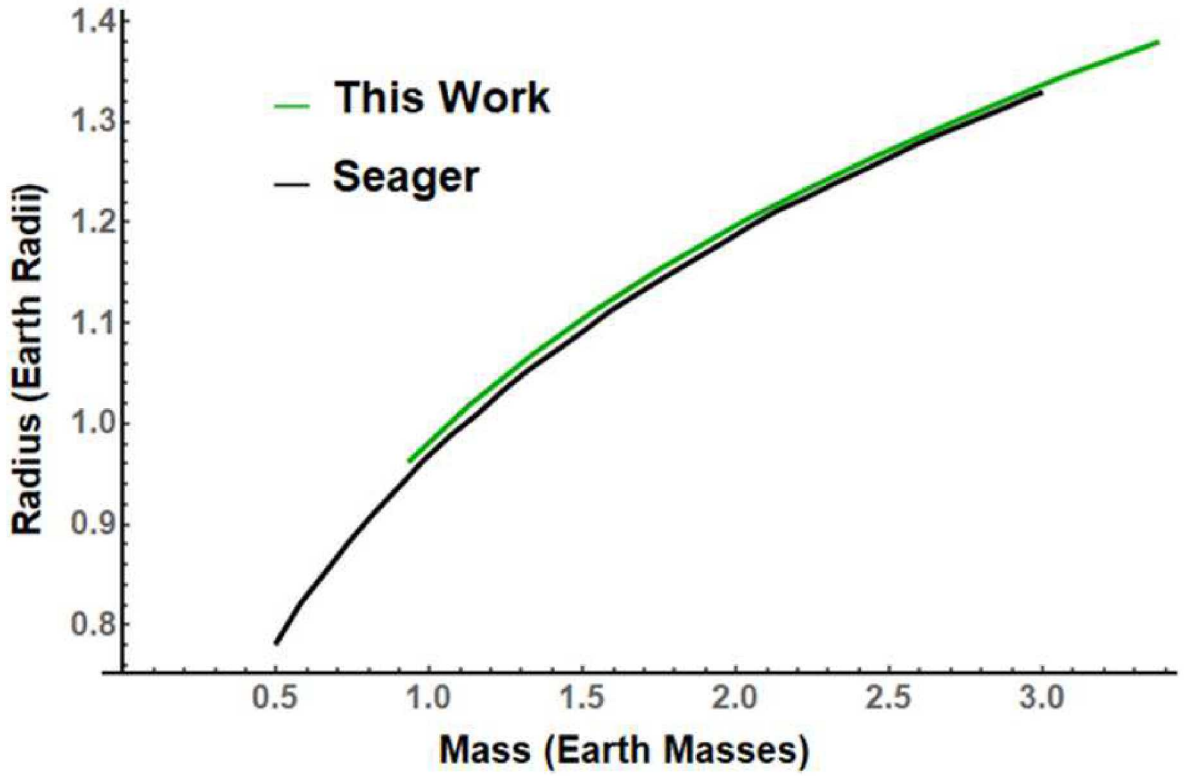

Conclusions and Future Work

Conclusion:

- We have performed shock-ramp experiments on Sandia National Laboratories' Z Machine to evaluate the equation of state of liquid iron along an elevated isentrope near Earth core pressure and temperature conditions.
- The results agree well with the SESAME 92141 table, validating its accuracy in this parameter region.
- We provide fit parameters for a new analytic EOS for liquid iron.
- We create radial models of planets and analyze their internal structure in the context of potentially life-supporting planets
- We have made significant advances towards a new specular reflection diagnostic on the Z machine for the study of electrical conductivities.

Future Plans:

- To improve modeling accuracy, we are performing similar experiments on iron alloys

Acknowledgements

Sandia:

- **The many people of Z operations**
- **DICE team:** Randy Hickman, Nicole Cofer, Keith Hodge, and Josh Usher
- **MSTS:** Sheri Payne and Richard Hacking
- **Design Engineers:** Andrew Maurer, James Williams, Lynn Twyeffort, John Fisher
- **Managers:** Christopher Seagle, John Benage, and Dawn Flicker
- **SEERI Program:** Trish St. John and Kristy Martinez
- **Z Fundamental Science Program**

Our fit matches most of the existing experimental data to within 2 GPa

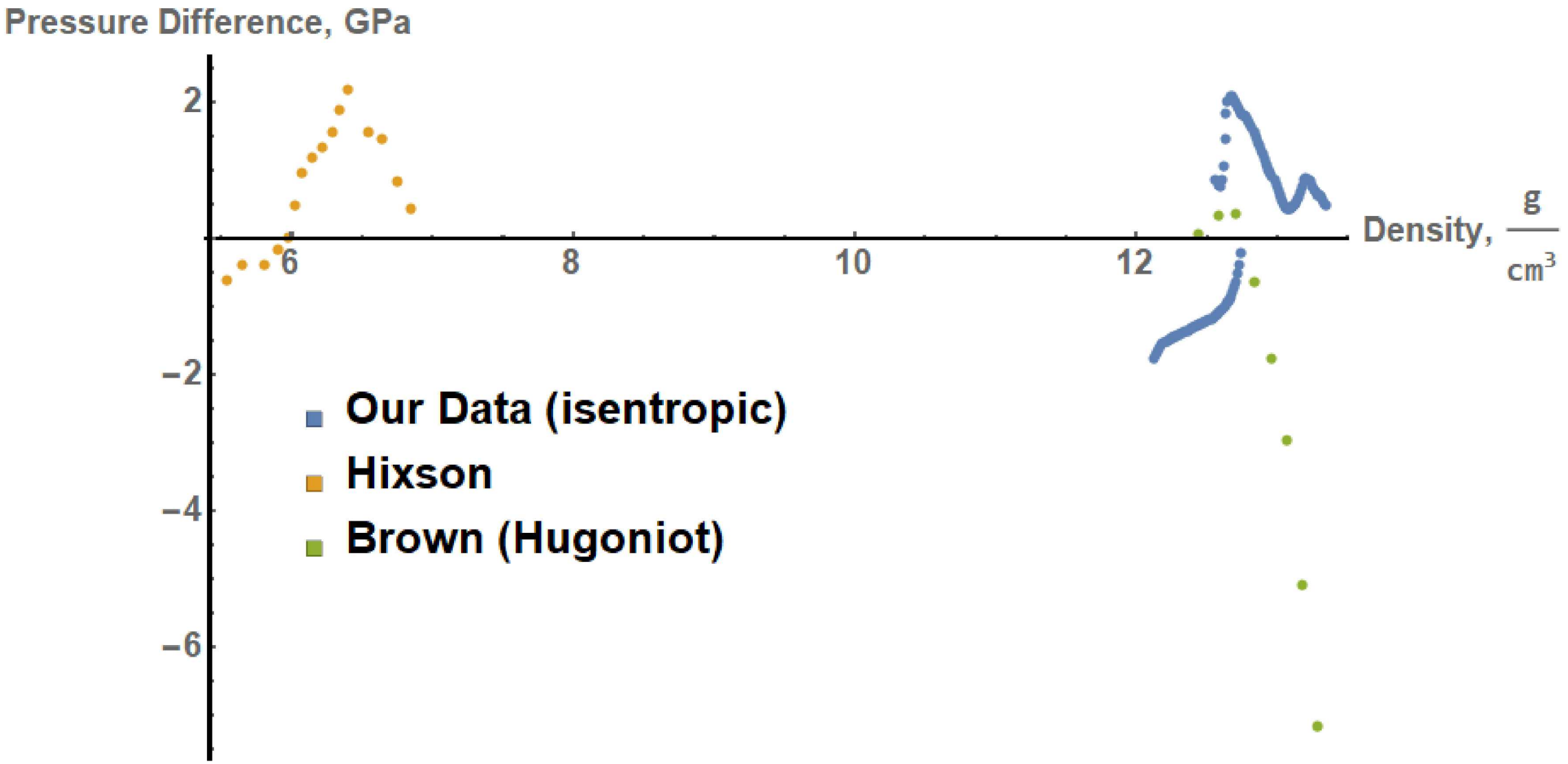

Thus we obtain an EOS surface for liquid iron

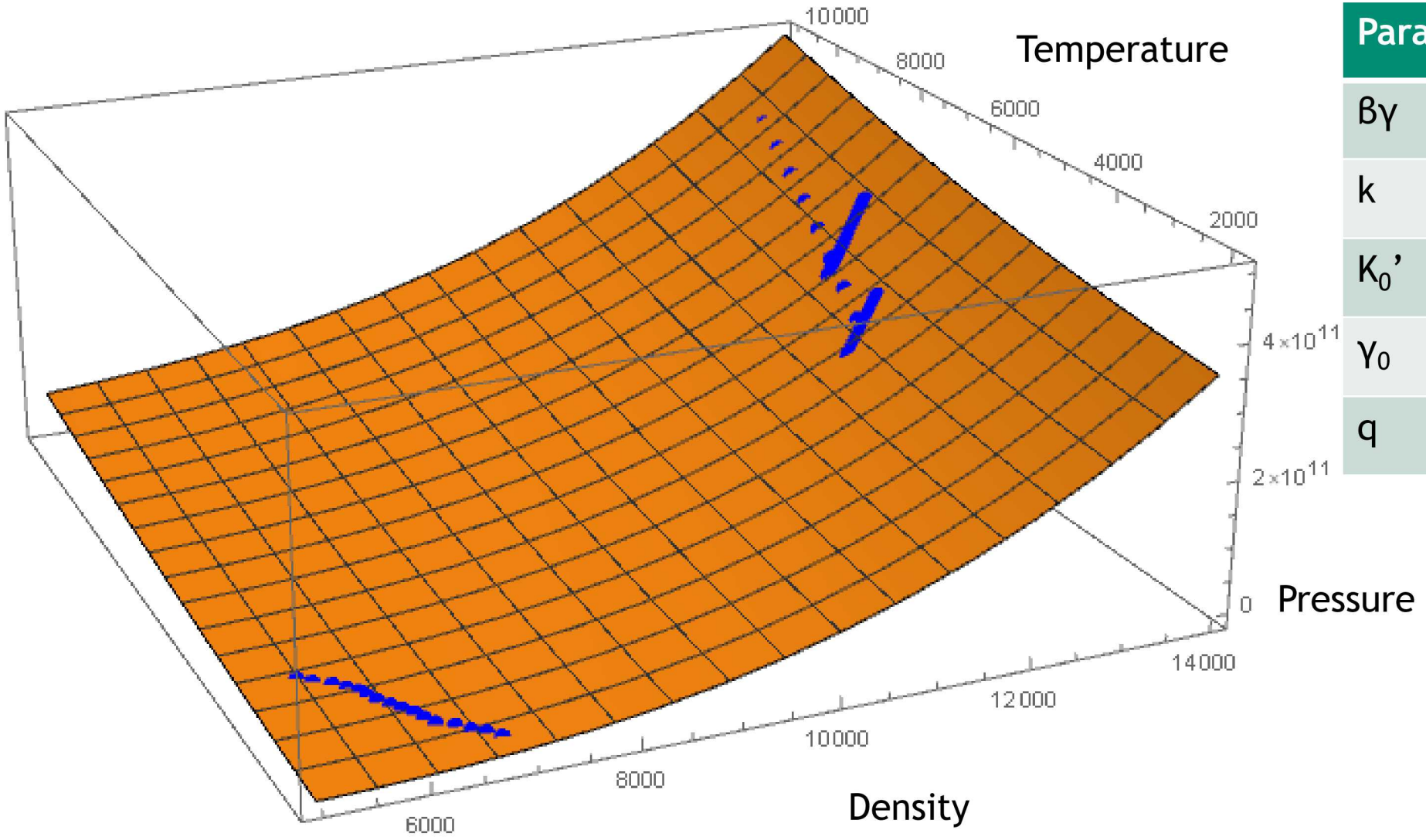

Parameter	Value
βγ	0.15 ± .1
k	0 ± 0.8
K_0'	5.1 ± 0.1
γ_0	1.03 ± 0.71
q	0.91 ± 0.43

Thus we obtain an EOS surface for liquid iron

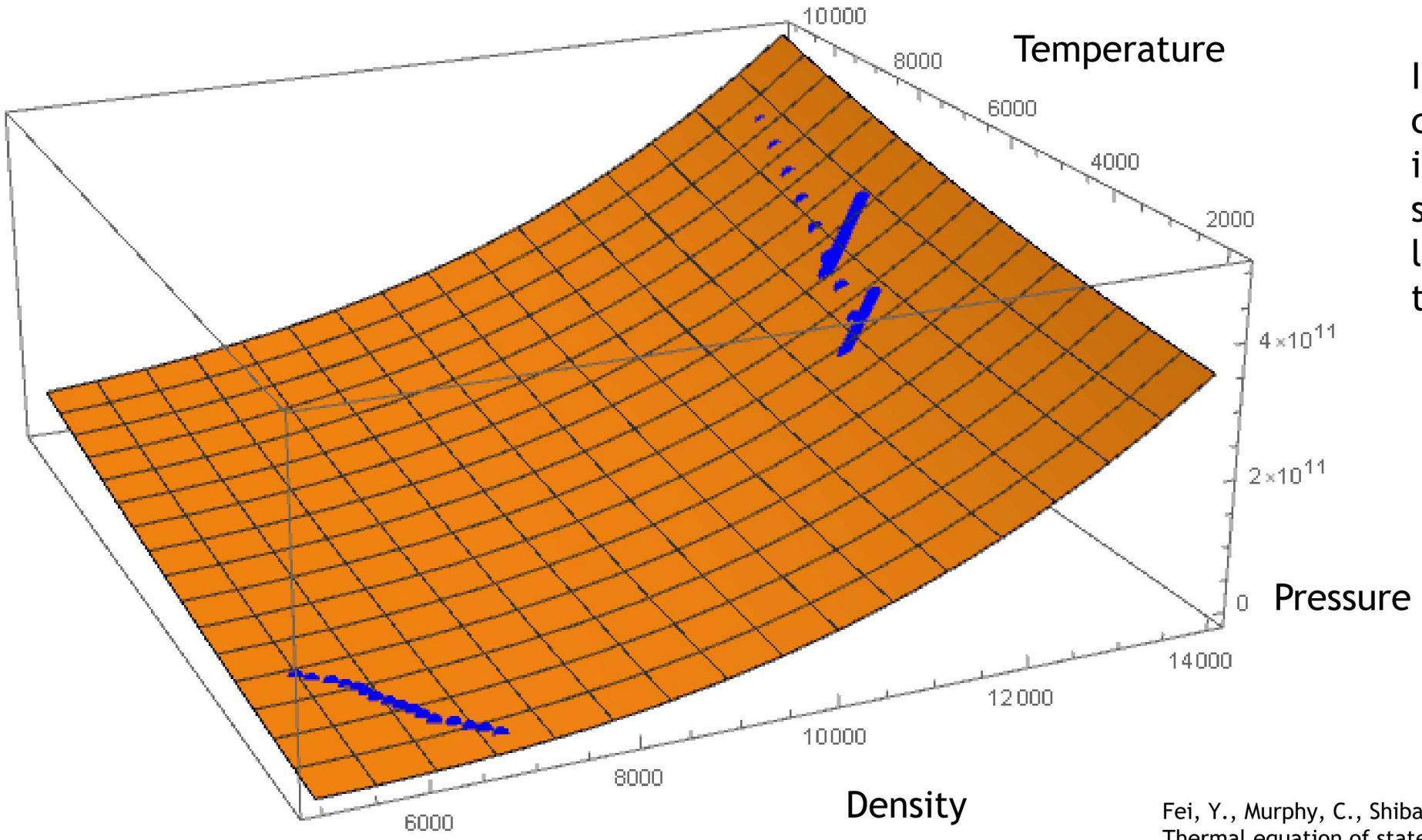

In comparison to a similar curve generated for solid iron by Fei et al., our surface is ~10 GPa (~3%) lower at the conditions of the Earth's core.

Fei, Y., Murphy, C., Shibazaki, Y., Shahar, A., & Huang, H. (2016). Thermal equation of state of hcp-iron: Constraint on the density deficit of Earth's solid inner core. Geophysical Research Letters, 43(13), 6837-6843.